THE KINGDOM OF THAILAND

THE PRE-FEASIBILITY STUDY
ON
SAN KAMPAENG GEOTHERMAL DEVELOPMENT PROJECT

FINAL REPORT

MARCH, 1988

JAPAN INTERNATIONAL COOPERATION AGENCY

THE KINGDOM OF THAILAND THE PRE-FEASIBILITY STUDY ON SAN KAMPAENG GEOTHERMAL DEVELOPMENT PROJECT FINAL REPORT MAR, 1988 J I C A

THE KINGDOM OF THAILAND

THE PRE-FEASIBILITY STUDY
ON
SAN KAMPAENG GEOTHERMAL DEVELOPMENT PROJECT

FINAL REPORT

MARCH, 1988

JAPAN INTERNATIONAL COOPERATION AGENCY

1716

PREFACE

In response to the request of the Government of the Kingdom of Thailand, the Japanese Government has decided to conduct a survey on the San Kampaeng Geothermal Development Project and entrusted the survey to the Japan International Cooperation Agency. The JICA sent to Thailand a survey team headed by Dr. Hisayoshi Nakamura of Japan Metals & Chemicals Co., Ltd. from July, 1982 to December, 1987.

The team, with the cooperation of the officials concerned of the Government of Thailand, conducted a field survey on geology, geochemistry, geophysics and heat flow and carried out exploratory drilling with a view to assessing geothermal potentiality in San Kampaeng area. After the team returned to Japan, further studies were made and the present report has been prepared.

I hope that this report will serve for the geothermal development in Thailand and contribute to the promotion of friendly relations between our two countries.

I wish to express my deep appreciation to the officials concerned of the Government of the Kingdom of Thailand for their close cooperation extended to the team.

March, 1988

Kensuke Yanagiya

Kensuke Yanagiya
President
Japan International Cooperation Agency

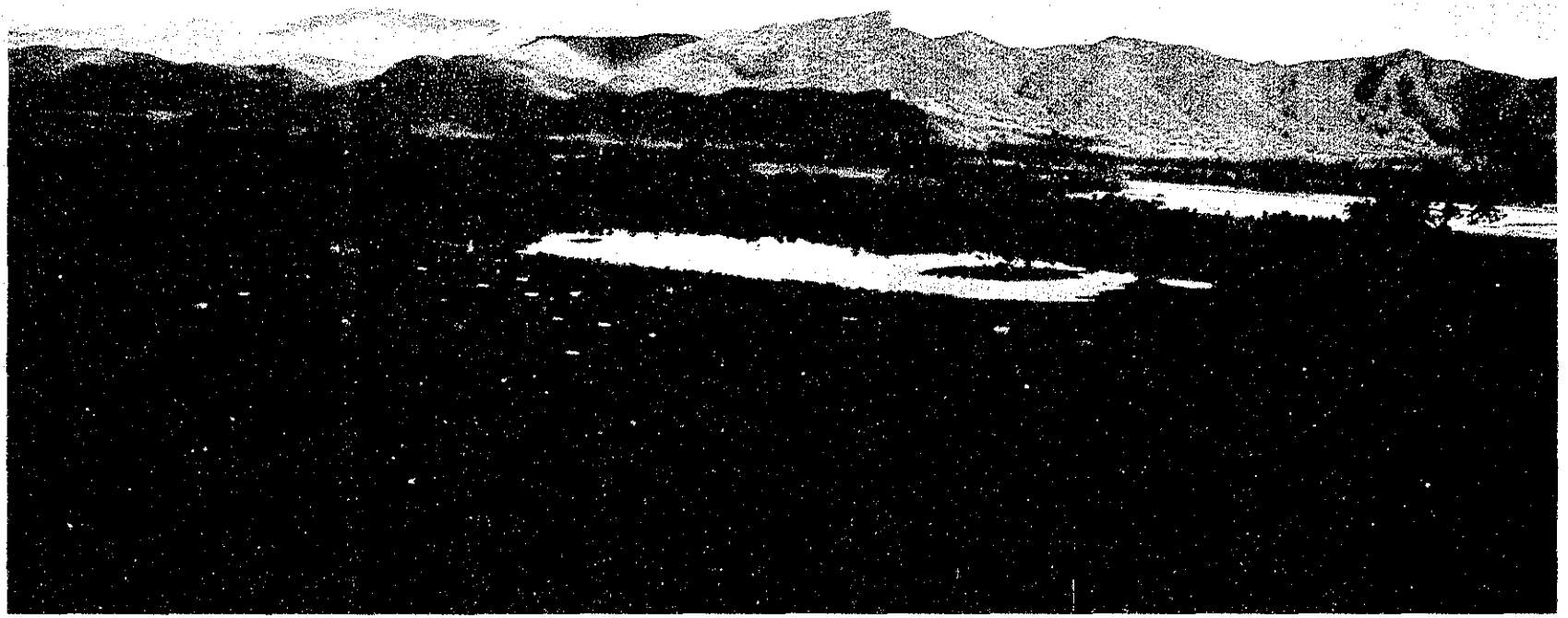

San Kampaeng Area

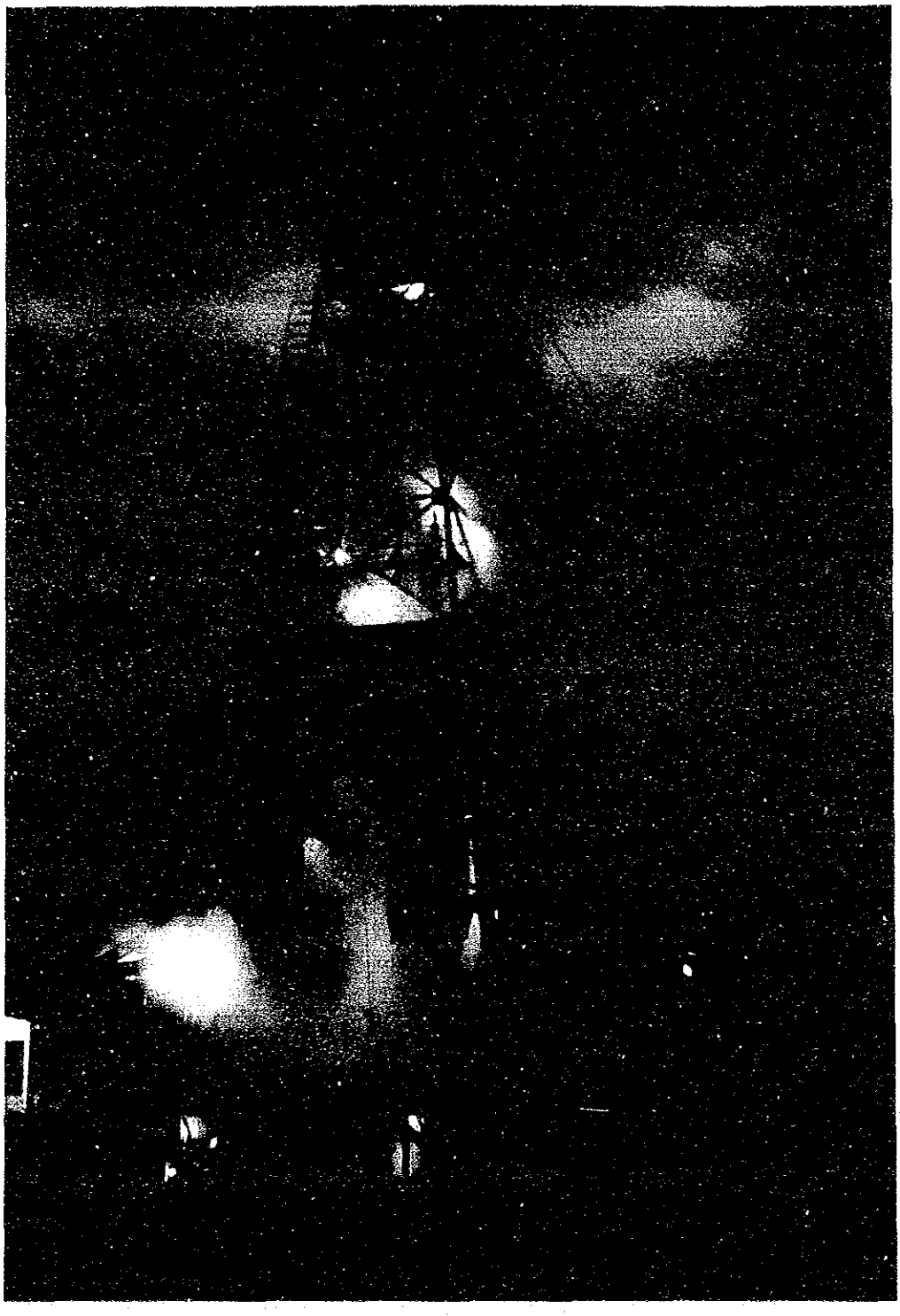

Producing fluid from GTE-8

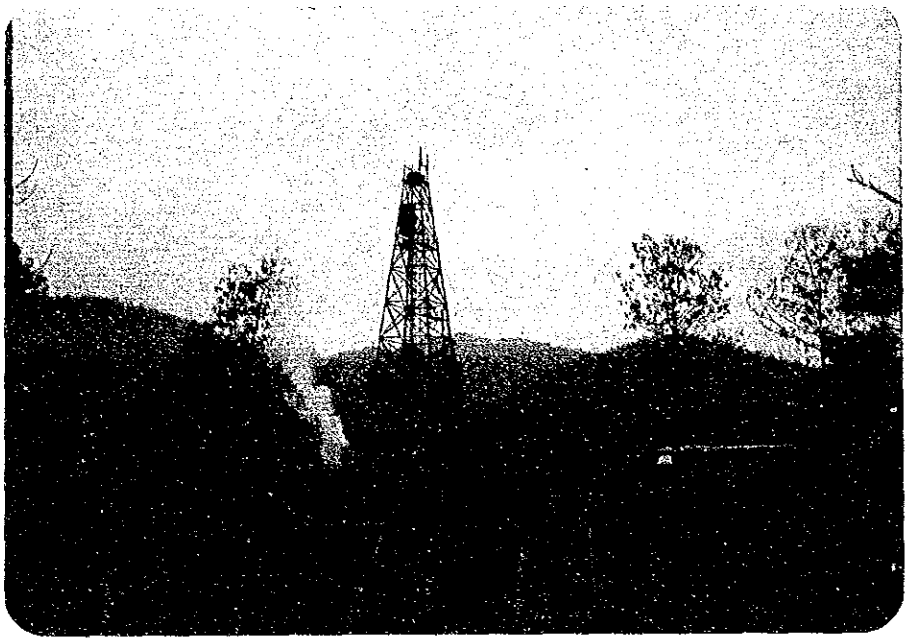

Drilling Site of GTE-7

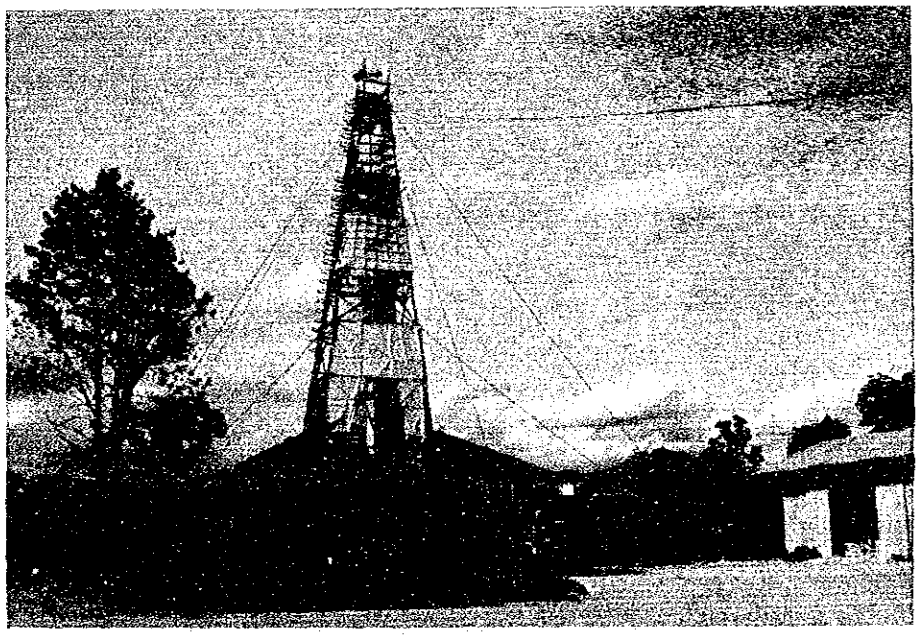

Drilling Site of GTE-8

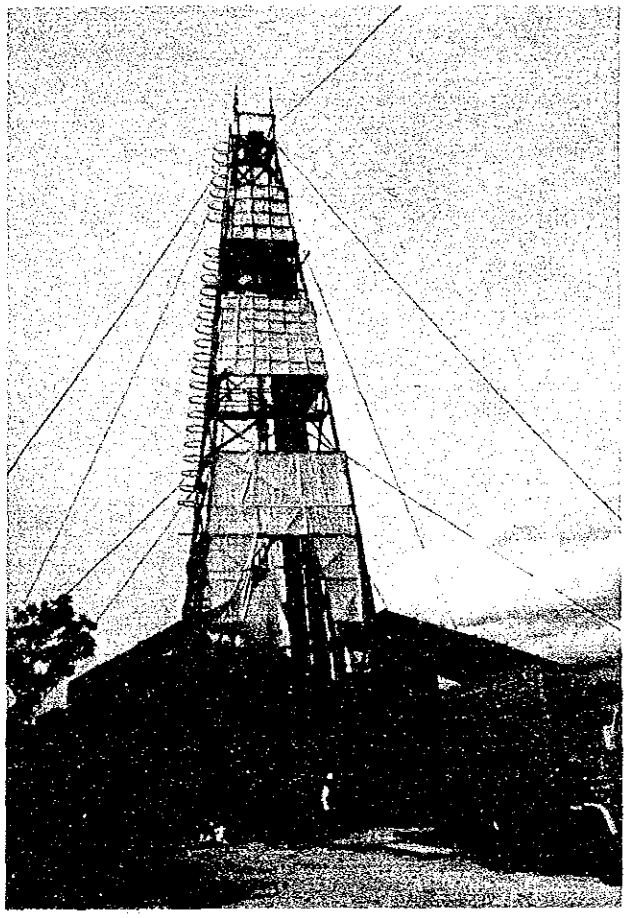

Logging in Production of GTE-8

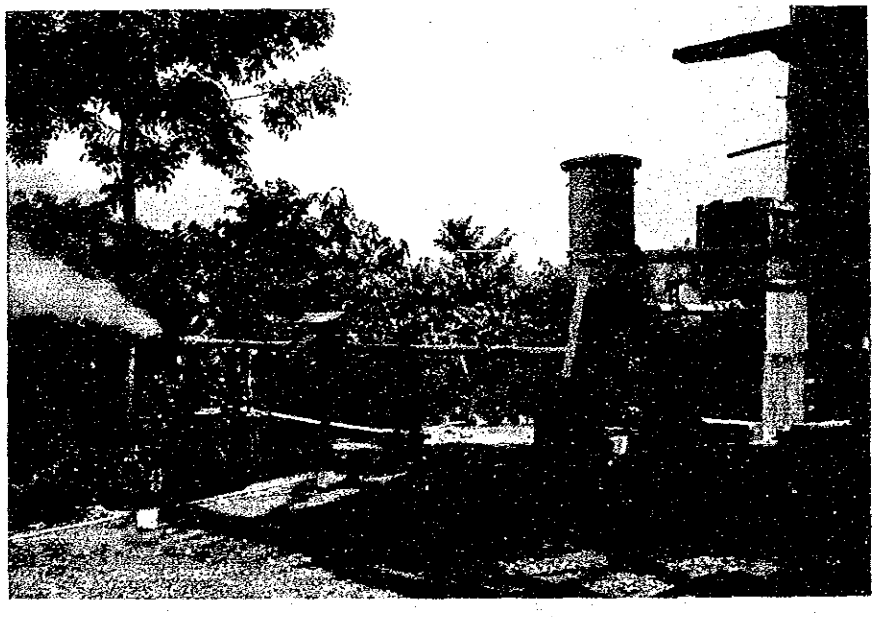

Piping Line of Characteristic of Flow Rate of GTE-8

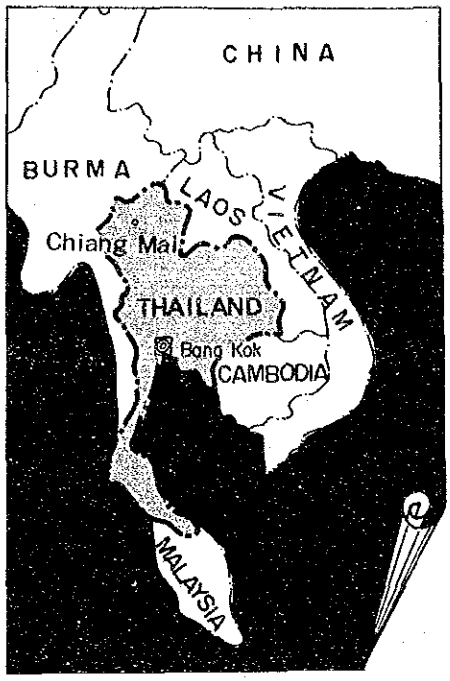

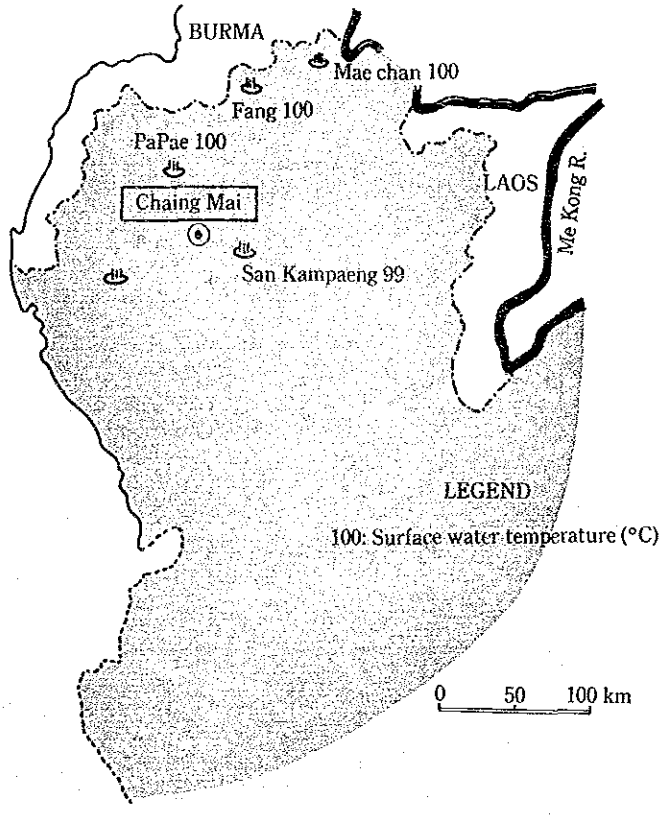

Distribution Map of Geothermal Areas in Thailand

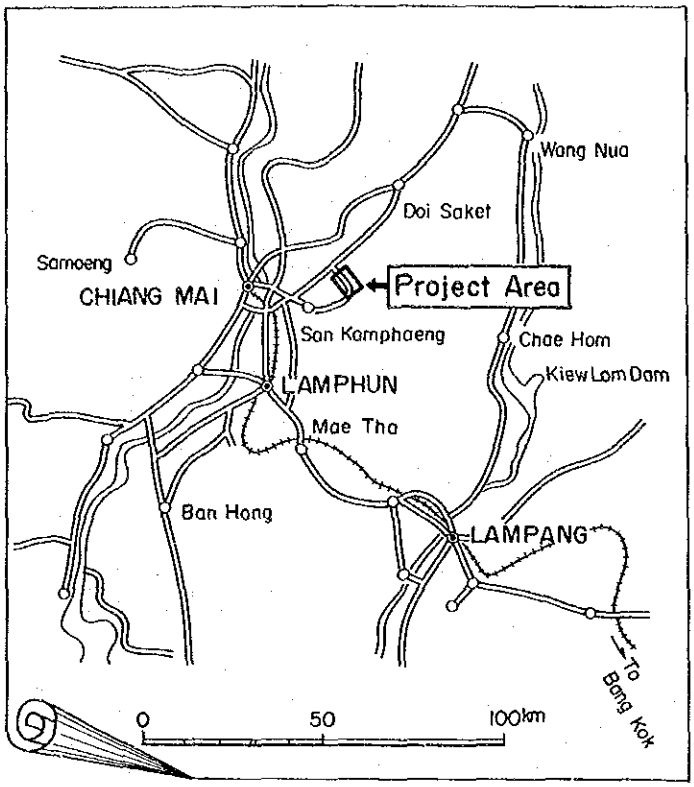

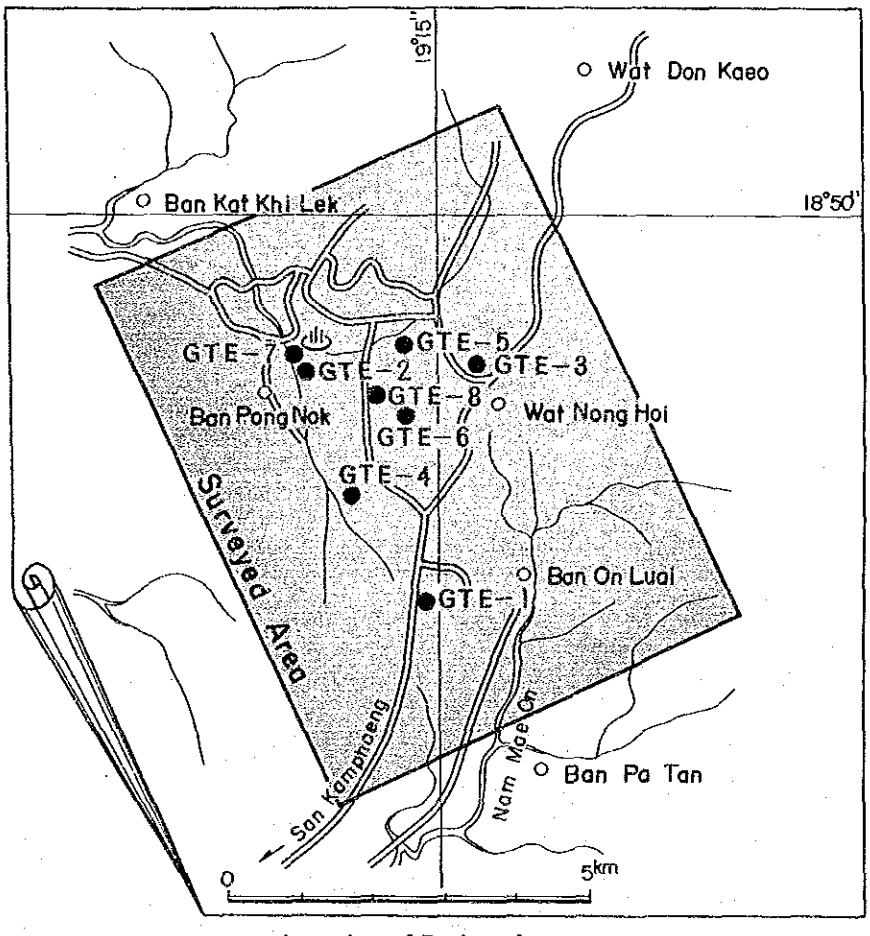

Location of Project Area

CONTENTS

List of Fig.

CONCLUSION

CONCLUSION

JICA carried out the pre-feasibility study on geothermal development in the San Kampaeng area in close cooperation with EGAT for six years from 1982. Since successful result was not obtained from drilling of the exploratory well, GTE-7,the survey period was extended for three years. However, from the results of drilling of GTE-8 which was undertaken by EGAT and production logging in GTE-8, information and data necessary for analysis of geothermal reservoir were collected. Thus, it became possible to evaluate the reservoir and check on possibility of geothermal development.

To summarize the results of survey, it would be possible in the San Kampaeng area to produce 1,000t/h of geothermal fluid keeping the pressure stable and to utilize this water for 5,000kW power generation by the binary-cycle system.

However, power generation by the binary-cycle system is at present less cost-effective than power generation by the various conventional systems unless consideration of multipurpose utilization. So, it is concluded that further detailed survey for geothermal development should be postponed until technology with ragards to the binary-cycle system is improved to a point where it can be applied economically in the San Kampaeng area.

Neverthless, the results of survey clarified the existence and extent of the geothermal reservoir and confirmed the capacity of the fluid supply to provide 5,000kW power generation. If EGAT would decide, in light of its long-term energy policy, to proceed with construction planning for a 3,000kW-5,000kW geothermal power plant by the binary-cycle system without placing sole priority on cost-effectiveness, it is recommended that subsequent survey be carried out according to the following steps:

i) There are three exploratory wells (GTE-2, GTE-6 and GTE-8) drilled in the geothermal reservoir area. Among them, only one well, GTE-8, was drilled to 1,000m and more in depth. Then,in order to examine the reservoir in detail, it is desirable to drill more exploratory wells with depth over 1,000m.
ii) Fluid temperature was estimated to show 160°C in depths by applying silica geothermometor method. However, fluid temperature in GTE-8 was 125°C at 900m level in depth, then, it is expected that the detected higher fluid temperature will be obtainable if another deep exploratory well is drilled at other location.
iii) The fractures were assumed to incline to east side from the results of drilling of GTE-2 and GTE-8. Considering fluid temperature and inclination of fractures, it is desirable to drill GTE-9 at the area nearer geothermal manifestation area and located at east side of axis line connecting the centers of the two highest underground temperature areas. Necessary depth of GTE-9 is 1,500m.
iv) If GTE-9 encounteres with many fractures as in the case of GTE-8, it is recommended that an additional well, GTE-10, is drilled at southeast of GTE-8 to confirm existence of fractures around there. By drilling of GTE-9 and GTE-10 as well as GTE-8, it is expected that geometory and extent of geothermal reservoir controled by distribution of fractures and fluid temperature become clear.
v) After completion of the above-mentioned drilling, it is necessary to carry out well logging and

production logging by means of the same method as that done in GTE-8, and also interference test between those wells. It is also recommended that supplementary geological survey is carried out in and around geothermal reservoir area.

Besides 3,000~5,000kW geothermal power development, construction of a 200~300kW demonstration power plant using geothermal fluid emitted from GTE-8 at present is proposed. This is due to the following reasons:

1) Among the non-volcanic countries in the world, there is no country where geothermal power plant has been constructed. Therefore, construction of geothermal power plant in the San Kampaeng area, although output is on a small scle of 200~300kW, will demonstrate the capability of geothermal development in a non-volcanic country.
2) Recently, the survey area with geothermal manifestations has been developed as resort area. In the last few years, hotels and restaurants were prepared in the area and number of visitors is increasing day by day. So, the power plant will be attracted by the visitors.
3) Generated electric power can be used for power source in the hotels and restaurants.
4) Besides power generation, exhausted hot water from the power plant has still water temperature above 60°C, then multipurpose utilization of hot water is available in this area. As the water can be used for wide areas such as industrial, agricultural, medical care and recreation, it is expected that utilization of hot water will contribute to economic development of this area. For this reason, it is desirable to promote utilization of hot water actively in future.
5) From the reasons mentioned above, it can be said that it is worth to construct a 200~300kW geothermal power plant using geothermal fluid from GTE-8 in the San Kampaeng area.

The proposal for constructing a small scale of power plant is due to idea that it makes practical application of the results of survey. However, as in the case of 3,000~5,000kW power generation, cost-effectiveness of geothermal power plant with respect to a large hydro and conventional thermal power system can not be expected unless the socio-economic benefits are also considered. Therefore, EGAT would evaluate the priority of such a scheme from standpoint of long-term energy policy. If EGAT would accept proposal for constructing a small scale of power plant in the San Kampaeng area, it is desirable to design and construct the power plant within the limit of amount of production of geothermal fluid which is emitting from GTE-8 at present because this would be the most direct and effective way to give benefit.

I. INTRODUCTION

I INTRODUCTION

1. Background of Survey

The Kingdom of Thailand has no active volcanos, but more than sixty hot spring areas in the country. Especially in northern Thailand, there are about twenty high temperature hot spring areas. Among them, boiling springs are found in the San Kampaeng, Fan, Mae Chan, Pa Pae and Mae Cheam areas. The Government of the Kingdom of Thailand has given attention to development of geothermal resources in the country as substitutional energy resources for petroleum. From 1977, the Electricity Generating Authority of Thailand (EGAT), Chiang Mai University (CMU) and the Department of Mineral Resourcese (DMR) organized a survey team and carried out reconnaissance survey of the geothermal resources in the hot spring areas. From the result of the reconnaissance survey, San Kampaeng and Fan were selected as further detailed survey areas.

This pre-feasibility study has been carried out in the San Kampaeng area by the Japan International Cooperation Agency (JICA) in response to the request from the Government of the Kingdom of Thailand, and in cooperation with EGAT, CMU and DMR. The objective of the survey was to evaluate the geothermal reservoir and the possibility of geothermal development based on the result of analysis of the geothermal reservoir in the San Kampaeng area.

As planned, first phase survey to understand gencaral geological structure, and second phase survey to select a drilling site of a JICA exploratory well were carried out in 1982. Also, analysis of the collected data and determination of a drilling site of the exploration well were included in the second phase in 1983. In the third phase, drilling of the JICA exploratory well and integrated evaluation of the geothermal field were planned to be carried out in 1984. Originally, the survey was planned to come to end after submit of a final report in 1984. However, because of the following reasons, the survey was extended over three years to 1987.

(1) The maximum temperature of the JICA exploratory well (GTE-7) was unexpectedly low and from the result of analysis of temperature distribution in the well, it was found that the drilling site is in a recharge area of a geothermal system. Accordingly, necessary information and data for evaluating the geothermal reservoir could not be obtained.

(2) In order to accomplish the objective of the survey, it was necessary to extend the survey period and to carry out a supplementary survey. With the coopcration of EGAT, it was decided to carry out fault tracing survey and underground temperature survey as the supplementary survey.

(3) As a result of the supplementary survey, existence of a geothermal reservoir was detected, and EGAT decided to drill an exploratory well (GTE-8) to confirm the existence of the geothermal reservoir. GTE-8 was drilled to a depth of 1,049.84m and flow characteristics test and production logging were carried out during drilling to obtain data necessary for reservoir analysis.

Although the survey period of the feasibility study was extended for three years, its objective was accomplished by utilizing GTE-8 drilled by EGAT. Thus, the survey was concluded with submit of a final report which includes reservior analysis and evaluation of possibility of geothermal development.

From the result of evaluation of fluid temperature, it was concluded that geothermal fluid in the San Kampaeng can not be used for geothermal power generation by steam, but has sufficient temperature for power generation by the binary-cycle system. Judging from capacity of fluid supply from the geothermal reservoir, it is expected that 5,000kW power generation will be obtained.

Recently, the San Kampaeng area has been developed as a resort area, so, for making practical application of the result of survey, it is desirable to construct a small scale of demonstration plant with output of 200-300kW by utilizing geothermal fluid emitting from GTE-8 at present. Electric power generated by the plant can be used for power source of the resort area, and then multipurpose utilization of hot water exhausted from the the power plant is available in this area.

2. Purpose of Survey

The Survey was carried out by the Japan International Cooperation Agency (JICA) in cooperation with the Electricity Generating Authority of Thailand (EGAT), Chieng Mai University (CMU), and the Department of Mineral Resources (DMR), in compliance with the request of the Government of the Kingdom of Thailand. The survey includes geological survey, geophysical survey, and drilling of one exploratory well in the San Kampaeng area, northern Thailand. The purpose of the survey is to evaluate potential of geothermal reservoir and to study feasibility of geothermal development in the area.

3. Outline of Survey Area

The survey area is located in San Kamapeng, Chiang Mai State, northern Thailand and about 30km east of Chiang Mai City, with the area of about 50km^2, lying between latitudes of 18°45′ and 18°50′N and between longitudes 99°13′ and 99°17′E.

Geothermal manifestations with many high temperature hot springs are distributed in the northwestern part of the survey area placed between Wat Pong Hom and Ban Pong Nok.

Two mountain ranges run with N-S direction in the survey area. They are the Doi Luang Mountains (elevation, 500m to 650m) in the west of the survey area and the Mae Tha mountains (elevation, 500m to 800m) in the south of the survey area. Between these two mountain ranges, there extends a plain of several kilometers wide with elevation of 350m to 400m.

4. Outline of Progress of Survey

The pre-feasibility study is divided into three phases.

The first phase survey comprised geological survey, gravity survey, magnetic survey to understand geological structure, andpreliminary test of well logging equipment in the test well. The first phase survey was carried out in 1982.

The second phase survey was carried out in the beginning of 1983. The survey consisted of seismic survey and deep electrical survey (MT method) to recommend a drilling site for an exploratory well. The results suggested that a geothermal reservoir might exist in the Bang Pong Nok area near the western mountains. In order to decide a location for drilling of an exploratory well, supplementary deep electrical survey by MT method was carried out in 1983.

The third phase survey in 1984 was scheduled to confirm existence of a geothermal reservoir and to evaluate it. The survey comprised drilling of a 1,500m deep exploratory well (GTE-7), collecting of cores and logging of the well.

Because rock was very hard, drilling of the well was terminated at a depth of 1,227.34m. The well encountered with only a few fractures and temperature at the bottom of the well was only 99.8°C. Potential of geothermal reservoir in the San Kampaeng area could not be evaluated from this well.

Therefore, in order to identify the geothermal reservoir, as a supplement of the third phase survey, fault-tracing survey and 100m-depth temperature survey were carried out by cooperation of EGAT in 1985. From the result of the supplementary survey, the data to show extent of the geothermal reservoir were obtained. Then, it was decided that EGAT would drill an exploratory well (GTE-8) to evaluate the geothermal reservoir.

EGAT carried out drilling of GTE-8 during 1986 and 1987. Drilling was terminated at a depth of 1,049.84m in December 1987. The well encountered with many fractures and emitted geothermal fluid. In order to collect basic data necessary for analysis of the geothermal reservoir, production logging and flow characteristics study were carried out under the condition of emission of geothermal fluid supplied from the fractures existing between 915m and 930m.

The pre-feasibility study of geothermal development in the San Kampaeng area was completed in 1987 with compilation of a Final Report.

5. Progress and Period of Survey

The survey was carried out between 1982 and 1987. Progress and period of survey are shown in Tables 1 and 2.

6. Members of Study Team

The members of the JICA Study Team and Thai counterparts are shown in Tables 3 and 4.

Table 1 Process of Survey

Item		1982												1983												1984												1985												1986												1987											
	Term	4	5	6	7	8	9	10	11	12	1	2	3	4	5	6	7	8	9	10	11	12	1	2	3	4	5	6	7	8	9	10	11	12	1	2	3	4	5	6	7	8	9	10	11	12	1	2	3	4	5	6	7	8	9	10	11	12	1	2	3
Primary Investigation	Geological survey																																																																
	Gravity survey																																																																
	Magnetic survey																																																														
	Logging of exploration Well and technical guidance																																																													
Secondary Investigation	Deep electrical survey																																																												
	Seismic survey																																																													
	Collection of the data of exploration wells																																																											
	Draft technical report																																																											
Secondary Investigation (Supplementary Investigation)	Deel electrical survey																																																											
Tertiary Investigation	Drilling of GTE-7																																																											
	Well logging of GTE-7																																																											
	Coring of GTE-7																																																											
Tertiary Investigation (Supplementary Investigation)	Rig down guidance																																																											
	Additional geochemistry survey																																																											
	Drilling heat holes and temperature logging																																																											
	Interim Report																																																											
	Well logging																																																											
	Deep electrical survey																																																											
	Seismic survey																																																											
	Supervise of Drilling of GTE-8																																																										
	Geological survey of GTE-8																																																										
	Well logging of GTE-8																																																										
	Production logging of GTE-8																																																										
	Measurement production flow rate of GTE-8																																																										
	Analysis																																																										
	Final Report																																																										

Legeno: Field survey; Integrated Analysis; Presentation of report; Work of EGAT

Table 2 Period of Survey

Item	Period	Field Survey	Analysis
Primary Investigation	Geological survey	From July 6, 1982 to Aug. 5, 1982 31 days	From Aug. 6, 1982 to Mar. 31, 1983
	Gravity survey	From Nov. 1, 1982 to Dec. 28, 1982 58 days	From Jan. 4, 1983 to Mar. 31, 1983
	Magnetic survey	From Nov. 1, 1982 to Dec. 28, 1982 58 days	From Jan. 4, 1983 to Mar. 31, 1983
	Logging of exploration well and technical guidance	(First) From July 28, 1982 to Aug. 16, 1982 20 days (Second) From Jan. 23, 1983 to Feb. 1, 1983 10 days	
Secondary Investigation	Deep electrical survey	From Jan. 4, 1983 to Feb. 22, 1983 50 days	From Jun. 1, 1983 to Sep. 30, 1983
	Seismic survey	From Jan. 4, 1983 to Mar. 31, 1983 87 days	From Apr. 1, 1983 to Sep. 30, 1983
	Collection of the data of exploration wells	From Jun. 15, 1983 to Jun. 24, 1983 10 days	
	Draft technical report	From Oct. 17, 1983 to Oct. 23, 1983 7 days	
Secondary Investigation (Supplementary Investigation)	Deep electrical survey	From Jan. 10, 1984 to Feb. 8, 1984 30 days	From Feb. 15, 1984 to Mar. 20, 1984
Tertiary Investigation	Drilling of GET-7	(Pre-Investigation) From May 9, 1984 to May 18, 1984 10 days (Drilling) From Jun. 5, 1984 to Mar. 8, 1985 261 days	From Mar. 11, 1985 to Mar. 23, 1985

Item \ Period		Field Survey	Analysis
Tertiary Investigation	Well logging (GTE-7)	(Testing) From Jun. 21, 1984 to Jun. 29, 1984 9 days (First) From Jan. 7, 1985 to Jan. 16, 1985 10 days (Second) From Feb. 25, 1985 to Mar. 8, 1985 12 days	From Mar. 11, 1985 to Mar. 23, 1985
	Coring (GTE-7)	From Feb. 12, 1985 to Mar. 8, 1985 25 days	From Mar. 11, 1985 to Mar. 23, 1985
Tertiary Investigation (Supplement Investigation)	Rig down guidance	From Aug. 26, 1985 to Sep. 21, 1985 27 days	
	Additional geochemistry survey	From Oct. 28, 1985 to Dec. 5, 1985 39 days	From Dec. 23, 1985 to Feb. 8, 1986
	Drilling of heat holes and temperature logging	From Aug. 5, 1985 to Oct. 15, 1985 72 days	
	Interim report	From Mar. 11, 1986 to Mar. 15, 1986 5 days	
	Well logging	–	From Sep. 3, 1985 to Sep. 20, 1985
	Deep electrical survey Seismic survey	–	From Sep. 3, 1985 to Oct. 7, 1985
	Supervise (Drilling of GTE-8)	(First) From Nov. 10, 1986 to Mar. 20, 1986 131 days (Second) From May 25, 1987 to Dec. 23, 1987 213 days	–
	Geological survey (GTE-8)	(First) From Mar. 4, 1987 to Mar. 20, 1987 17 days	

Item \ Period		Field Survey	Analysis
Tertiary Investigation (Supplement Investigation)	Geological survey (GTE-8)	(Second) From Oct. 4, 1987 to Oct. 20, 1987 17 days	
	Well logging (GTE-8)	From Mar. 4, 1987 to Mar. 20, 1987 17 days	—
	Production logging (GTE-8)	From Oct. 4, 1987 to Oct. 20, 1987 17 days	—
	Measurement production flow rate (GTE-8)	From Oct. 11, 1987 to Oct. 20, 1987 10 days	—
	Final Report	From Feb. 29, 1988 to Mar. 4, 1988 5 days	From Aug. 20, 1987 to Sep. 19, 1987 From Nov. 2, 1987 to Nov. 24, 1987 From Jan. 5, 1987 to Jan. 23, 1987 From Feb. 23, 1988 to Feb. 25, 1988

Table 3 List of Members of Study Team

Survey	Investigation	Name of member	Position
Leader	Primary ~ Tertiary	Hisayoshi Nakamura	J. M. C.
Geological survey	Primary ~ Tertiary 〃 〃	Kensuke Wakabayashi Yukhichi Tagami Toshio Ide	MINDECO MINDECO J. M. C
Gravity survey	Primary	Mikio Kimura	MINDECO
Magnetic survey	Primary ~ Tertiary	Fukujiroh Miyoshi	MINDECO
Well logging	Primary and Tertiary Primary ~ Tertiary	Takao Takeyama Kosei Obara	Kaihatsu Kogyo Co., Ltd. J. M. C
Production logging	Teriary	Kohsei Obara	J. M. C
Deep electrical survey	Primary ~ Secondary Primary ~ Tertiary 〃	Kazuhisa Nobuchi Shinji Takasugi Sumio Seki	J. M. C J. M. C J. M. C
Seismic survey	Primary ~ Secondary 〃 〃 〃 〃 Secondary ~ Tertiary 〃	Akira Aribe Kazuyoshi Nohara Kohji Kowamura Toshimichi Suzukawa Takashi Hori Shinji Takasugi Sumio Seki	Ube Industries Co., Ltd. Ube Industries Co., Ltd. Ube Industries Co., Ltd. Ube Industries Co., Ltd. Ube Industries Co., Ltd. J. M. C J. M. C
Drilling	Tertiary 〃 〃 〃 〃 〃	Hisashi Uemura Sakari Kon Kyuya Fujii Shohei Kusano Etsuo Hatakeyama Hidenori Fujinuki	N. M. C N. M. C N. M. C N. M. C N. M. C N. M. C
Additional geochemistry survey	Tertiary 〃 〃	Kiyohisa Shibata Munehiro Fukuda Toshio Ide	MINDECO MINDECO J. M. C
Measurement production flow rate	Tertiary	Yukio Fujii	J. M. C

J. M. C : Japan Metals and Chemicals Co., Ltd.
MINDECO : Mitsui Mineral Development Engineering Co., Ltd.
N. M. C : Nittetsu Mining Consultants Co., Ltd.

Table 4 List of Member of Thailand-side Counterpart

Survey	Name of member	Position
General affairs	Mr. Chaya Jivacata	EGAT
	Mr. Chai-Asa Bhotirungsiyakorn	EGAT
	Mrs. Amara Atibodhi	EGAT
	Dr. Kamol Takabut	EGAT
	Mr. Kiatichai Patikornsilp	EGAT
	Mr. Songkeat Limsiri	EGAT
	Mr. Chayant Nakswat	EGAT
	Mr. Somchai Wongpornpaxdee	EGAT
	Prof. Tavisakdi Ramingwong	CMU
	Mr. Amnuaychai Tienprasert	DMR
Geological survey	Mr. Surachai Praserdvigai	EGAT
	Mr. Adichat Surinkum	DMR
	Mr. Prapat Sophonpongphipat	DMR
Geophysical survey	Mr. Surachai Praserdvigai	EGAT
	Mr. Visit Coothongkul	EGAT
	Mr. Precha Laochu	DMR
	Mr. Pairoj Pangpolsumrit	DMR
	Mr. Wanchai Prasartkhetwittaya	EGAT
	Mr. Suebsak Solgosoom	DMR
	Mr. Suthep Lertsrimongkol	EGAT
Well logging	Mr. Jirakom Patumanond	EGAT
	Mr. Buncha Kongsupapkul	EGAT
	Mr. Ekachai Sinratanpakdee	EGAT
	Mr. Pramual Wongpunga	EGAT
	Mr. Sommart Siri	EGAT

Survey	Name of member	Position
Drilling	Mr. Wanchai Silapanon	EGAT
	Mr. Puchong Chinpongsanond	EGAT
	Mr. Surachai Praserdvigai	EGAT
	Mr. Wanchai Prasartkhetwittaya	EGAT
	Mr. Udom Kunarak	EGAT
	Mr. Songsak Bhaddee	EGAT
	Mr. Patana Hutakorn	EGAT
	Mr. Tanit Songchan	EGAT
	Mr. Prasert Kidchalard	EGAT
	Mr. Pratueng Nokyoongtong	EGAT
	Mr. Sompis Boonpairote	EGAT
	Mr. Phadung Dangkongko	EGAT
	Mr. Thavorn Jangsri	EGAT
Chemical survey	Mrs. Nitiya Petchpaibool	EGAT

List of member of other cooperative

Speciality	Name of member	Position
Geochemist	Associate Prof. Benjavun Ratanasthien	CMU
Geologist	Assistant Prof. Charn Tantisukrit	CMU
Geophysist	Associate Prof. Kitichai Wattananikorn	CMU
Geologist	Assistant Prof. Surapong Lerdthusnee	CMU

EGAT: Electricity Generating Authority of Thailand
DRM : Department of Mineral Resources
CMU : Chiang Mai University

II. RESULTS OF FIELD SURVEY

II. FIELD SURVEY AND RESERVOIR EVALUATION

1. REGIONAL SURVEY

1.1 Geological Survey

1.1.1 Generalization

(1) Geological Setting of the Kingdom

Including the San Kampaeng geothermal area, the northern part of the Kingdom of Thailand occupies the central area of the Indochina peninsula. Geology of Southeast Asia can be outlined as follows;

Table 1.1-1 Geological Outline of the Southeast Asia

Structural Zone			Area	Age
Himalayan Orogenic Zone			Western half of Burma, Andaman Is., Sumatra Is., Java Is.	Cretaceous ~ Quarternary
Indo-Chinese Platform	Indosinia	Indosinian Orogenic Zone	Indochinese Mountain Range (Southern China, North-east Burma, Laos, Vietnam, most of Thailand, Malayan Pen.)	Permian ~ Jurrasic (mainly Triassic)
	Annamia	Helsynian Orogenic Zone	Indochina, peninsular (Northeast Thailand, Laso, Cambodia, Vietnum)	Late Palaeozoic (mainly carboniferou)
	Kraton	Metamorphic Basements	– do –	Pre-Cambrian ~ Early Palacozoic

The oldest rocks (basements) of the Indochina peninsula are metamorphic rocks (gneiss, granitic rocks of Palaeozoic age) formed by the orogenic movement occurring during the late Pre-Cambrian or early Palaeozoic. These rocks are distributed in the area of the Kontum Plateau of southern Vietnam, the Hong River basin of northern Vietnam, the Myitkyina district of north Burma and west Chiang-Mai of north Thailand forming old stabilized Kraton (Fig. 1.1-1).

Starting from the central Kraton of the area, three orgenic belts, namely the Helsynian orogenic belt of Carboniferous age, the Indosinian orogenic belt of mainly Triassic age and the Himalayan orogenic belt of Cretaceous to Quaternary are successively developed moving outward from the area, suggesting that the new geologic formations have functioned to enlarge the continent.

The Helsynian orogenic belt covers the eastern part of the Indochina peninsula forming the Annamia massive. The Indosinian orogenic belt is distributed widely in the Indochina peninsula forming the Indosinian massive.

The orogenic belts, together with basement metamorphic rocks form a stable geologic unit called the Indochinese Platform.

The Himalayan orogenic belt is distributed in Burma and extends to the Andaman sea at the

South, continues to Sumatra and Java, and joins the Borneo and the Philippine Islands portion of the greater circum-Pacific Himalayan orogenic belt. The Himalayan orogenic movement induced the Indosinian block to form gentle undulation and faulted block movements. The northern part of the Kingdom of Thailand a portion of the above mentioned geological setting of Southeast Asia, is geologically divided into four (4) geo-structural units (Fig. 1.1-2), namely from west to east: the West Tectonic Province, the Main Western Range Tectonic Province, the Central North Tectonic Province and the East Tectonic Province.

The West Tectonic Province is west of Mae Sot and Mae Sariang and is the western-most area of Thailand. Geology of the province is mainly composed of thick carbonate rocks and clastic rocks ranging in age from Carboniferous to Jurrasic, No volcanic rocks are observed. The area is located in the faulted subsiding belt in which thick Quaternary freshwater sedimentary sequence is developed and reaches 300m in thickness.

The Western Range Tectonic Province includes the main mountainous region of Thailand between Mae Sariang and Chiang Mai. Geology of the tectonic province is composed of two major units, namely Pre Cambrian meta-sediments intruded by arch-shaped granite and weakly metamorphosed early palaeozoic continental shelf deposits which unconformably overlay the granite. This tectonic province is entirely characterized by the uplifting block movement caused by faulting.

The Central North Tectonic Province covers a wide north-south trending zone in central Thailand. It starts from Chiang Rai in the north and continues to Chanthaburi via Uttarait. Geology of this tectonic province is composed of volcanic rocks of calc-alkaline rock series ranging in age from middle Palaeozoic to early Mesozoic and sedimentary rocks of continental facies. This province is characterized by strong and clear folding structures and thrust faults.

The East Tectonic Province is represented by the Khorat Plateau of northeast Thailand. Geology of this province is mainly composed of thick "red beds" with evaporites formed during the late Triassic to Cretaceous suggesting a terrestrial sedimentary environment on the continent. Folding structure in the province is not clear.

The geological environment of northern Thailand with relation to geothermal resources will be outlined hereunder. All of the geothermal fields of northern Thailand are located in the stabilized Indosinian orogenic belt forming the back area of the Himalayan orogenic belt. These fields are affected by gentle folding and faulted block movements caused by the Himalayan orogenic movement.

The San Kampaeng geothermal field is located at the north-western border of the central North Tectonic Province in the orogenic belt. Influence of Himalayan progeny and existence of granite are the two important factors in terms of the genesis of geothermal fields of northern Thailand (Fig. 1.1-3).

The Himalayan orogenic belt in this area was formed as a result of collision between the Indian plate and the Eurasia plate. The Himalayan orogenic belt, except for the Burmese area, has a characteristic zonal geo-structural arrangement featuring from west to east subductional trench, volcanic island arc and marginal sea (expanding small marine area). This geo-structural setting suggest that the Indosinian orogenic belt, to which the geothermal field of northern Thailand belongs, is under regional compressional stress caused by subduction of the Indian plate. However, the influence of the local tensional stress resulting from spreading of the Andaman sea should be taken into consideration in interpreting the geology of the area.

The axis of spreading trend in the Andaman sea is NE-SW, and is cut by NS faults with right-hand lateral movement. Although minor dislocation of axis and weakening intensity of spreading can be expected, the axis of spreading possibly extends to northern Thailand. The tensional stress field formed by spreading may cause deeply penetrating fractures, and ascending high temperature mantle material accompanied by high heat flow in the area.

Northern Thailand, compared with other areas, has a rather wide distribution of granite, especially in the Main Western Range Tectonic Province and Chiang Rai area, close to Burmese border, in the Central North Tectonio Province. Most of the hot-springs are distributed in and around the granite area. The San Kampaeng area also can be considered as adjoining such area of Triassic granite distribution. This suggests a genetic relationship between hot-springs (geothermal area) and the existence of granite.

Nevertheless, the precise genetic relation between geothermy and granite is still uncertain. However, two possibilities can be hypothetically assumed: one, that the granite works as the heat source, and two, the granite serves to transfer hot fluid from deeper area.

In the case of granite working as a heat source, heat is derived from decay of radioelements. The heat produced from granite in Thailand is three times higher than that of granite in southwestern Japan. Supposing the thickness of the granitic layer as 10km, the calculated heat flow of the area may reach 1.2HFU. Granite is distributed widely in the area, and considering the huge quantity thereof in the earth crust, the roll of granite as the heat source may be considerable in northern Thailand.

Generally the highest temperature of hot springs in the granite area is around 60°C ~ 70°C. Hot springs where temperature reaches up to 90°C ~ 100°C, such as Fang and San Kampaeng, are exceptional. Accordingly, the genesis of geothermy in northern Thailand is geologically interpreted as resulting from ascending mantle material under similar spreading conditions to that of Andaman sea, and producing a regional high heat flow area. Also, the accumulated heat of decay in the granite of Carboniferous and Triassic may play an important roll as a heat source in the area.

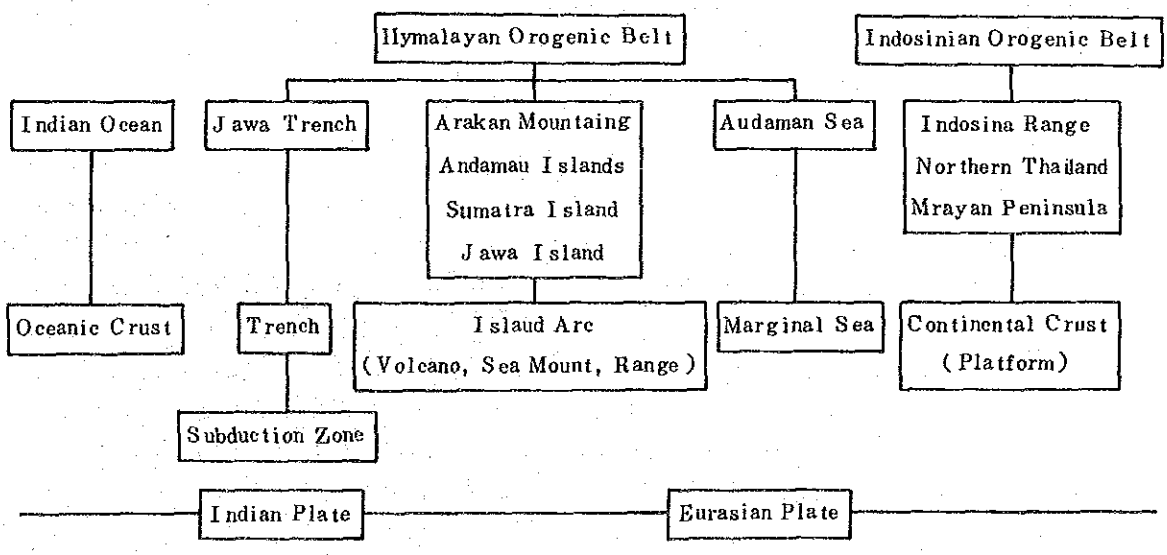

Fig. 1.1-3 Schematic Relationship between Hymalayan Orogenic Belt and Indosinian Orogenic Belt

(2) Outline of the Survey

The geological survey was carried out in the San Kampaeng area to study the geo-structural conditions of the geothermal reservoir by crarifying lithofacies, stratigraphy, geological ages and geo-structure of the area and also, by elucidating the genetic relation between the geology and the geothermal features (geothermal manifestations, distribution of alteration zones, etc.) on the basis of survey results obtained.

The geological survey was conducted over a 95km route covering an area of approximately 50km^2. Topo-maps of 1:10,000 were used as base mapping for the field survey along the main route and alteration zone survey. In important areas such as areas of geothermal manifestation, ground survey was employed to prepare large scale topo-maps for conduction detailed geological survey.

Samples collected during the field survey were studied with regards to lithology in the laboratory by microscope, paleontologic analysis (Table 1.1-2), absolute age determination (Table 1.1-3) and X-ray diffraction analysis (Table 1.1-4). Thin sections were studied under the microscope to determine minerals and rock composition. Paleontologic study on fossiliferous limestone revealed Fusulinid fossils useful to determine geological age. Absolute age determination on basalt and granite was done by K-Ar method. X-ray diffraction analysis was conducted on the hydrothermally altered rocks from the areas of geothermal manifestation to determine alteration minerals. On the basis of field survey and the laboratory data, geological maps, geological profiles and the zonal distribution map of alteration zonings were prepared. The lithology of the area, stratigraphy, geological age and geologioal structures of the formations underlying the area were clarified, and the relationship between geo-structure and geothermal manifestations including hydrothermaly altered zone was identified.

1.1.2 Stratigraphy

The rocks underlying the surveyed area are composed, in ascending order, of Carboniferous Mae Tha Formation, middle Permian Kiu Lom Formation in the Ratoburi Group, Triassic granites and Alluvium deposits. (Fig. 1.1-4)

(1) Mae Tha Formation

This formation is distributed in the western mountainous area as well as in the east of the eastern mountainous area, and is mainly composed of compact, hard, white-colored medium-grained massive sandstone. Thin intercalation of dark colored shale is observed in the eastern area. Microscope examination reveals that rocks are composed mainly of round to sub-angular sand grains, 0.1 ~ 10 mm in diameter, of quartz and sericitized feldspar, although large grains over 1.0 mm in diameter are contained in some cases. This formation is the basement in the surveyed area, and is fault contacted with the upper Kiu Lom Formation. No stratigraphical relation of the two formations is observed. The thickness of this formation is estimated to be more than 1,600 meters, although the upper and the lower limits are not confirmed.

(2) Kiu Lom Formation

The Kiu Lom Formation is distributed widely in the NNE-SSW trending central zone of the

surveyed area with fault contact to the Mae Tha Formation on both sides. The formation is divided lithologically into three units; lower sedimentary rocks, middle limestone and volcanics and upper volcanics.

The lower Kiu Lom Formation is divided into the following members in ascending order.

i. Alternation of limestone and shale
ii. Sandstone
iii. Alternation of siltstone, sandstone and chert
iv. Chert
v. Alternation of siltstone and sandstone
vi. Andstone

The lowest alternation of limestone and shale is composed mainly of light grey to dark grey limestone and black shale with intercalated grey sandstone layers. The limestone of this alternation yields Fusulinid fossils of Neoschwagerina, Sumatrina etc. showing age of middle Permian.

The sandstone, second to the lowest member, is represented by white medium grained sandstone exposed in the hilly area in the northwest of Wat Pong Hom.

Alternation of siltstone, sandstone and chert is distributed in the area from Ban Pong Hom to the Huai Ang river in the western part of the surveyed area, and from Nam Mae On to Nam Hae Lai in the eastern part. This alternation is composed mainly of siltstone inserted with sandstone and chert.

Chert bed is distributed in the area from Ban Pong Hom to the east of the Huai Ang river. This bed is composed mostly of chert, but intercalation of siltstone is observed in the lower part while layers of sandstone and siltstone are intercalated in the upper part of this bed.

Alternation of siltstone and sandstone is distributed in the area from Bank Pong Hom to the Huai Ang river. This alternation is composed mainly of siltstone with intercalated sandstone layers.

The uppermost sandstone bed is distributed in the area from the east of Ban Pong Nok. The rocks composing this sandstone bed are massive, and hard, white, medium-grained sandstone.

The middle part of Kiu Lom Formation is divided into two members: the lower basaltic member of lava and tuff and the upper member of limestone and shale.

The lower basaltic lava and tuff layers are distributed around Ban Mae Khu Ha and the northern and southern vicinities thereof. The basaltic lavas occur as seated beds with thickness of 5 to 10 meters in the basaltic tuffs.

The lavas are dark to deep green, vesicular and massive. The overlying limestone and shale are distributed along the small and S-shaped north-south trending hilly land in the central part of the surveyed area. The limestone is generally massive and thin black shale layers are intercalated in some places. Although fossils yielded from the limestone are limited, the occurrence of Schubertella sp., and Kahleria indicates the age of middle Permian.

The upper part of the Kiu Lom Formation is composed of basaltic lava, tuff, lapilli tuff and tuff breccia, with intercalated thin layers of tuffaceous sandstone, chert and siltstone.

The basaltic lava is deep to dark green in color, vesicular and massive, with thickness varying from several to 20 meters, and with good continuation. The results of K-Ar dating are rather scattered showing values of 389±19 m.y., 206±10 m.y., 190±10 m.y., and 119±14 m.y. This spread in results may be caused by alteration after effusion. Also, the effusive environment of the

lava may contribute to the dispersed results.

(3) Granitic Rocks

Granitic rocks are distributed in the area east of Bank Huai Kaeo in the northeastern part of the surveyed area. Lithology of the granite is porphysitic biotite granite with large phenocryst of feldspar. K-Ar dating is 212±10 m.y. suggesting intrusion during the late Triassic (Table 1.1-3).

(4) Alluvium

Along the Nam Mae On river in the central to southern part of the surveyed area, and along the streams near Ban Pong Hom in the northwestern part of the surveyed area, alluvium deposits are well developed and the land is utilized for rice field. The alluvium is composed of clastic deposits derived from the surrounding area. The thickness is estimated to be less than 10 meters in most parts.

Table 1.1-3 K-Ar Age Determination of Igneous Rocks

Sample Number	Rock Name	Locality	Mineral	Age (m.y.)	Ar^{40} Rad SCC/gm x 10^{-5}	Ar^{40} Rad%	K %
W-006	Basaltic Welded tuff	Wat Don Kaeo	Whole Rock	119 ± 14	0.024 0.024	12.7 20.8	0.05 0.05
W-009	Pyroxene Basalt	Wat Nong Hoi	Whole Rock	389 ± 19	0.067 0.068	42.3 36.9	0.04 0.04
W-017	Pyroxene Basalt (Altered)	Huai Hat	Whole Rock	206 ± 10	0.836 0.852	89.7 91.2	0.99 1.00
T-103	Biotite Granite	Ban Huai Kaeo	Biotite	212 ± 10	2.84 2.90	81.2 86.6	3.27 3.31
T-107	Pyroxene Basalt	Ban Mae Koha	Whole Rock	190 ± 10	0.751 0.751	88.4 90.1	0.96 0.97

The constants for the age calculations are: $\lambda_\beta = 4.96 \times 10^{-10} yr^{-1}$,
$\lambda = 0.581 \times 10^{-10} yr^{-1}$, $^{40}K = 1.167 \times 10^{-4}$ atom per atom of natural potassium.

1.1.3 Geological Structure

(1) Geo-structural Characteristics

The surveyed area is divided by the main faults into three structural units: the Doi Luang uplifted zone, the Ban Pong Hom subsided zone and the Mae Tha uplifted zone (Fig. 1.1-5). The faults bordering the three units are the Huai Pong fault and the Huai Mae Koen fault, both of which are normal faults trending in NNW-SSE direction (Fig. 1.1-6).

The Doi Luang uplifted zone geomorphologically corresponds roughly with the western mountainous area. This uplifted zone is composed of massive sandstone of the Carboniferous Mae Tha Formation. Faults with trends of NW-SE, E-W and N-S are well developed in this zone. Foldings with axes in the NW-SE are also recognized.

The Ban Pong Hom subsided zone corresponds with the central lowland. In the western part of this subsided zone, sedimentary rocks (sandstone, shale, limestone and chert etc.) of the middle to lower part of the Kiu Lom Formation of the Permian period are distributed. The eastern part

is occupied by basaltic lava and pyroclastic rocks of the upper part of the Kiu Lom Formation. Faults with trends of NNE-SSW, NNW-SSE and NW-SE are well developed in this zone. Although folding structures are recognized in some parts with the axes in the same directions as the major faults, geological structure in this zone is monoclinal to the east as a whole. The dipping of the beds is generally as steep as 50° to 80°.

The Mae Tha uplifted zone corresponds with the eastern mountainous area. This uplifted zone is composed of sandstones of the Mae Tha Formation, shales of the lower part of the Kiu Lom Formation, and granite intruding the Mae Tha Formation. Faults of NNW-SSE trend are prevailing, but there are some faults trending in NE-SW or E-W direction, being cut by the former faults. Also, foldings with axes in the N-S or NW-SE direction are developed. Thus, the Doi Luang uplifted zone and the Mae Tha uplifted zone show good similarity in terms of the lithofacies of the component rocks and the characteristics of the geological structure.

(2) Fissure System

In this surveyed area, there are many faults of various trends such as NNW-SSE, NNE-SSW, NW-SE, NE-SW and NE-SW. Among them, the faults trending NNN-SSE are the most significant in relation to the geological structure. The above mentioned Huai Pong fault and Huai Mae Koen fault are two of these significant faults. The three faults with trend of NW-SE, recognized from Ban Pong Nok to the upstream area of the Huai Ang river, are considered to be faults branching from the Huai Pong fault. The fault planes of the faults in this area including the Huai Pong fault and the Huai Mae Koen fault are rarely observable. However, as the extension of the faults on the surface is straight in many cases, it is inferred that they have quite steep dipping angles and that they are probably normal faults.

There are other tectonic fractures in addition to those stated above as well in the surveyed area. One type of these structural fractures are joints, which have been filled with quartz veins. The trends of these quartz veins are predominantly in E-W direction, most of which cross the folding axes, probably representing tensional cracks formed by folding.

It is recognized that the characteristics of the fissures and fractures differ depending on the lithofacies of the beds. That is, the quartzose sandstone of the Mae Tha Formation and the basaltic lava pyroclastic rocks of the upper Kiu Lom Formation are rather massive and less jointed. On the other hand, the alternation structure of sedimentary rocks of the middle and lower Kiu Lom Formation causes vertical heterogeneits. Although large-scaled jointing is less developed, fine jointings are highly developed, producing fine rock fragments. Especially, chert has high fragility and is often brecciated into small fragments. Also, siltstone weathers and alters easily, to form white and soft rock, containing mans fissilities.

(3) Folding Structure

Generally, folding structures are well developed in this area. Intensity and pattern of the foldings are different in each structural zone.

In the Doi Luang uplifted zone and in the Mae Tha uplifted zone, foldings have been formed close to one another, repeating synclines and anticlines with wave length of 400 meters to 1 kilometer. The folding axes are almost horizontal, showing trends of NW-SE or NNW-SSE. The dips of the beds are as gentle as 40° to 60°.

In the Ban Pong Hom subsided zone, folding structures are not marked, and isoclinal structure is characteristic, dipping 50° ~ 80° to the east. The folding structures recognized in the western central parts of this zone have horizontal to gently plunging folding axes, with the trend of NNE-SSW.

(4) Alteration Zone

The hydrothermal alteration zone was studied in an approximately 2 km^2 area around the area where the geothermal manifestations are distributed. X-ray diffraction analysis was conducted on the samples collected in this survey (Table 1.1-4).

The detected clay minerals are halloysite, montmorillonite, saponite, sericite, chlorite, kaolinite, and alunite. Gypsum, jarosite and pyrite are also recognized.

Based upon the assemblage of the clay minerals, alteration zones have been classified as follows: alunite zone, kaolinite zone, kaolinite montmolillonite zone, montmolillonite zone and halloysite zone (Fig. 1.1-7). Widespread clay minerals such as sericite and chlorite were excluded in studying the zonal arrangement in the area.

Alunite associated with saponite has been recognized only at a point about 30 meters south of the site where the geothermal exploration well GTE-2 is located. Accordingly, extension or distribution of the alunite zone is not obvious, although possibly it extends to the south.

The kaolinite zone extents east and west, around the site of GTE-2 and in the east-side area thereof. The zone is also recognized in the north of Ban Pong Hom and along the road at the foot of the mountains in the west. The kaolinite-montmorillonite zone is recognized around the hot spring about 80 meters northwest of GTE-2, and also about 400 meters east thereof. The zone extends east ~ west, adjacent to the northern boundary of the kaolinite zone.

The montmorillonite zone is recognized in and around the area where principal hot springs are distributed, along the Huai Mae Khu Ha River. The zone is approximately 200 meters wide and extends east and west.

The halloysite zone is recognized around Wat Pong Hom and about 400 meters southeast of Ban Pong Hom. The distribution of this zone extends in a E-W or NW-SE direction.

It is thought that assemblages of alteration minerals in the geothermal area are controlled by the chemical composition and the temperature of hydrothermal solution. The hydrothermal solution causing alteration in this area is thought possibly to be neutral to acidic liquid of 200°C temperature or less.

Zonal distribution of alteration is observed in the following order from the center towards the outside.

alunite zone
kaolinite zone
kaolinite-montmorillonite zone
montmorillonite zone
halloysite zone

This zonal distribution, from the alunite zone at the center toward the outer halloysite zone, suggests that the temperature of the hydrothermal solution has been decreasing, with the solution gradually changing from acidic to neutral.

The alteration zones are distributed in the east ~ west direction, and their distribution sug-

gests a change in characteristic of the solution from high temperature south of GTE-2 to lower temperature toward the north. Also, existing hot springs are distributed from the alunite zone to the montmorillonite zone, suggesting that the distribution of the alteration zones have intimate relation to the present activity of the hot springs. The alunite zone confirmed by this alteration survey suggests that the center of the hydrothermal alteration would be at the south of the point of GTE-2.

1.1.4 Geology and Down hole Temperature of Exploratory Wells

Many wells have been drilled for geothermal exploration in the San Kampaeng area. Major wells are 10m wells to measure ground temperature distribution and 100m wells (EGAT-1 to 15) and 500-1,000m wells (GTE-1 to GTE-8) to study geological structure and ground temperature distribution.

Geology and temperature in 500 ~ 1,000m wells are described as follows.

(1) Well Geology

1) GTE-1 (Fig. 1.1.-8)

① Location: Southeastern part of the survey area, 99°14′12″E and 18°46′22″N.

② Depth: 500m

③ Temperature: The maximum temperature of the well is 80.4°C at 462 m. Temperature gradient is 12.0°C/100 m. Temperature gradient is larger beyond 200m as a result of cooling by low temperature water infiltrating along numerous fractures at shallower depths. However, temperature versus depth curve is rather straight, which implies that heat conduction is dominant in heat flow.

④ Geology: Mainly composed of basaltic rocks of the upper Kiu Lom Formation. Lithology is grey green, basaltic lava and pyroclastics such as tuff and tuff-breccia. Pyroclastic members as predominant. Basaltic lava occurs at three horizons: 94m to 124.5m, 196m to 251m and 378m to 450m. Tuff is fine to medium grained basaltic tuff with intercalating tuff breccia. Flow structure and brecciated fractured fault zone are observed occasionally. Calcite vein and quartz vein are also observed. Chloritization is obvious in whole cores. High angle fracturing is dominant in shallow (less than 150m deep) formation while at the deep part of the well the amount of fracturing decreases, and the dip of fracturing becomes gentle.

⑤ Electrical log: Electrical logging measured resistivity and spontaneous potential. Correlation between resistivity and depth, lithology and temperature was not found. Resistivity is slightly higher at shallower than 80m and deeper than about 400 m.

2) GTE-2 (Fig. 1.1-9)

① Location: At the geothermal manifestation between Wat Pong Hom and Ban Pong Nok.

② Depth: 500m

③ Temperature: The well was drilled near a geothermal manifestation. Hot water outpours from the well.

Temperature in the well, measured immediately after drilling, shows a maximum value of 106°C at about 300m. Temperature decreases beyond 300m. However, when temperature

logging was carried out for the second time in February 1987' the maximum temperature was lower than before and temperature distribution was similar to a convection type. Because the well is artesian with outpour of hot water, temperature at the well head is high (66°C). The reason why temperature in the well became lower compared to that of immediately after drilling is the result of cooling effect of shallow ground due to the small amount of outflowing hot water at 300m.

④ Geology: Composed of sedimentary rock sequence of the lower Kiu Lom Formation, such as siltstone, shale and limestone and alternation thereof. Limestone occurs at three horizons: 195.1 m to 221.1 m, 267.3 m to 337.0 m and 430.8 m to 483.5 m. Calcite vein, quartz vein and pyrite dissemination are common. The carbonaceous shale at a depth of 230 m is fragile and easily fragmented.

⑤ Electrical log: Generally, limestone is resistive and lutace-ous rock is conductive. Spontaneous potential is inversely proportional to resistivity.

3) GTE-3 (Fig. 1.1-10)

① Location: Near Wat Nong Noi, about 2.5km east of GTE-2.

② Depth:

③ Temperature: Temperature logging is only to about 150m. Temperature at the bottom of the well is 60°C and temperature gradient is much smaller than for any other well.

④ Geology: Composed of basaltic rocks of upper Kiu Lom Formation. Basaltic tuff pale green to dark green in color, fine grained, compact, and less jointed is predominant. Basaltic lava, tuff breccia and thinly laminated tuff are intercalated. Alteration is not obvious except for a limited number of calcite veinings.

⑤ Electrical log: Resistivity varies greatly with depth. Generally, resistivity is high at shallow (shallower than 75m) level, and becomes lower with increasing depth. Correlation between resistivity distribution and lithology or alteration is not clear.

Spontaneous proportional to resistivity, with high resistivity peaks corresponding to low spontaneous potential peaks.

4) GTE-4 (Fig. 1.1.-11)

① Location: About 1.4km northwest of GTE-1.

② Depth: 500m

③ Temperature: 82°C at 440m.

Temperature of the well increases linearly with depth which implies heat conduction around the well. Temperature gradient changes at about 280 m. Shallower than 280 m gradient is 8°C/100 m (1°C/12.5 m) and becomes larger below 280 m to 18°C/100 m (1°C/5.5 m). The change occurs because heat conductivity of the geological formation changes (larger at shallow depth). Geological formation at shallow depth consists of tuff and andesite lava and at greater depth consists of alternation of sandstone and shale.

④ Geology: Rocks corresponds to the middle and the lower Kiu Lom Formation. Geology between the surface (0 m) and 302.5 m is mainly composed of andesitic tuff and basaltic andesite of middle Kiu Lom Formation with frequent alternation of sandstone and shale of lower Kiu Lom Formation at a depth of 302.5 m to 500 m.

⑤ Electrical log: The well was electrically logged to 140 m. Resistivity tends to be high in basalic andesite and low in tuff and reflects change of lithology. Spontaneous potential is

generally small and shows very little change. Therefore it cannot be correlated with lithology, alteration and fracture.

5) GTE-5 (Fig. 1.1.-12)

① Location: About 750 m northeast of GTE-2, and neighbouring a geothermal manifestation.

② Depth: 500 m

③ Temperature: 96°C at 500 m.

Temperature distribution of this well is of a typical heat conduction type. Temperature gradient is relatively large at 12°C/100 m (1°C/8.3 m). Complete lost circulation occurred at around 300 m. Above this point, temperature gradient was larger, while that below was relatively.

④ Geology: Composed of sedimentary sequence of lower Kiu Lom Formation. Alternation of sandstone and shale is located between 0 m to 131.0 m. Frequent alternation of chert, shale, sandstone, andesitic tuff and tuff breccia is found between 131.0 m and 240.0 m depth. This test well encountered heavy circulation loss considered to be caused by the fractured zone of the Ban Mae Khu Ha fault, or highly jointed rock (chert bed).

⑤ Electrical log: Resistivity varies greatly with depth. This is thought to be caused by regular alternation of shale, standstone and chert.

Spontaneous potential varies slightly with depth.

6) GTE-6

① Location: 690 m southeast of GTE-2.

② Depth: 489 m

(3) Temperature: 118°C at 485 m.

This is the first well where steam and geothermal water outpour occurred. No other well drilled before this well produced either. Temperature logging does not show true formation temperature. Temperature at the bottom of the well where fractures were encountered is 118°C and at the well head temperature is 103°C. Temperature difference between the well bottom and head is caused by cooling at shallow depth.

④ Geology: Generally composed of alternation of shale and sandstone. In the upper horizon (0 m to 230 m), shale is the dominant member of the alternation while in the lower horizon (230 m to 489 m), sandstone is dominant. The difference between the upper and lower horizons is not only the rock facies but the degree of alteration and the dip of stratification. In the upper horizon, dip is as steep as 70° ~ 80° and alteration is rather weak while in the lower horizon, dip es as low as 20 to 30° and alteration of quartz veining and silicification is remarkable. The test well GTE-7 drilled by JICA and GTE-8 drilled by EGAT will be described at clauses 3 and 5.

1.2 Gravity Survey

1.2.1 Generalization

(1) Gravity Measurement

Two gravimeters, G-283 and G-366 manufactured by LaCoste & Romberg Co., Ltd., were

used for gravity measurement (Table 1.2-1). The base station, No. 1,000, for the gravity survey was established on a concrete floor at the entrance of the dormitory for clinic staffs, at about 100 m west of the EGAT CAMP. The gravity value at the base station No. 1,000 was set to 978,947.981 mgal.

Gravity values were measured at a total of 230 stations over 50 km². Gravity stations are along survey lines cut by Thai crews, and neighboring roads and paths. Stations were located by topographic map of scale 1/10,000 or by topographic survey.

Table 1.2-1 Specification of Gravimeter

Name, type	La Coste & Romberg, INC. Model G Geodetic Gravity Meter	
No.	283	366
Measurement range	0 ~ 7,386.54 m-gal	0 ~ 7,404.56 m-gal
Temperature of thermostat cell	51.7°C	49.0°C
Reading line	2.80	2.90
Date of purchase	September 1971 (overwhole June, 1981)	September 1974
Size	14 x 15 x 20 (cm)	17 x 15 x 22 (cm)
Weight	8.6 kg	9.1 kg

(2) Leveling

Levels of the survey stations were measured by EGAT leveling crews. The leveling base station is the bench mark BMCS-18 (392.418m above sea level) at the EGAT CAMP.

(3) Collection of rock samples

Eighty four (84) rock samples were collected from the survey area and their densities were measured for a topographic correction of the observed gravity data and for interpretation of the gravity survey.

(4) Reductions of gravity data

All the collected gravity data were corrected for gravimeter drift, station elevation, influence of the earth tide, nearby topography and latitude (Fig 1.2-1).

(5) Compilation of gravity data

The gravity survey results were correlated with the existing gravity data surveyed by DMR. Neither survey used the same gravity base station or leveling base station. Therefore, for compiling the results of the two surveys, gravity values from the two surveys at identical points were correlated. When gravity data from both surveys were integrated, gravity data of the DMR survey which was collected from either stations nearby those of the team's survey or outside of the survey area, and from stations where isogravity lines showed erroneous curve where eliminated from compilation. Eighty seven (87) sets of gravity data obtained by the DMR survey were included in preparation of the Bouguer map.

(6) Density Measurement

Density value for topographic correction is inferred from density measurement of rook samples (Fig. 1.2-2, Table 1.2-2), G-H relation map (Fig. 1.2-3), and study of correlation between the topographic map and the Bouguer map. As a result of their study, the density for gravity correction was decided as 2.6 g/m³.

(7) Preparation of Bouguer map

The Bouguer map was prepared as follows:

① Corrected gravity values were computed from the collected gravity data.

② Gravity values at the grid points (150m × 150m) were calculated by the weighted polynomial fitting method.

③ Isogravity lines were drawn for the gravity values at the grid points.

(8) Filtering and two dimensional analysis

Because the Bouguer map contains many different wave lengths from anomalous bodies of different depths and different sizes, a third order residual map from third order trend analysis, a deep gravity component map and a shallow gravity component map from spectrum analysis were prepared (Fig. 1.2-4).

Two dimensional analysis was carried out by Talwani's method. Three sections, (A-A'), (B-B') and (C-C'), were analyzed.

1.2.2 Results of Survey

(1) Analytical plans and profiles

On the basis of analysis, the following plans and profiles were drawn up.

Bouguer Anomaly (ρ = 2.6 g/cm³) (Fig. 1.2-5)
Gravity trend
Residual Gravity (Fig. 1.2-6)
Deep Gravimetric Component (1,200 m)
Shallow Gravimetric Component (190 m)
Profile of Underground Structure (A-A') (Fig. 1.2-7)
Profile of Underground Structure (B-B') (Fig. 1.2-8)
Profile of Underground Structure (C-C') (Fig. 1.2-9)
Underground structure (Fig. 1.2-10)

(2) Density measurement

From the result of density measurement of rock samples, the rock densities in the surveyed area are divided as shown below.

High Density g/cm³

basaltio tuff, tuff breccia, lapilli tuff	..... 2.93	(The upper part of the Kiu Lom formation)
basalt	.....2.94	

Medium Density

limestone	2.72	(The middle part of the Kiu Lom formation)
sandstone	2.58	
granit	2.57	
quartz vein	2.62	

Low Density

shale	2.56	The middle of lower part of the Kim Lom formation)
sandstone	2.54	
chert	2.46	

(3) Outline of gravity distribution

From the Bouguer anomaly map (ρ = 2.6 cm^3), the highest value of isogravity countour is -2.25 mgals, while the lowest value is -12.25 gals.

The trend of isogravity countours is N-S as a whole. Especially, in the eastern extremity, in the central part and in the western extremity of the survey area, crowded distribution of the N-S trend isogravity contours is marked. In these areas, existence of faults are assumed by geological survey, such as the Huai Mae Koen fault, the Huai Mae Khu Ha fault, the Ban Mae Khu Ha fault and the Huai Pong fault.

(4) Gravity gradient

Gravity distribution in the survey area is approximated by a third order polynomial to express regional gravity gradient.

The highest gravity zone is around Ban On Klang, the east of the survey area, and a high gravity zone extends north Ban Nong Hoi. In the wester part of the survey area, a low gravity zone extends N-S direction centered by Huai Pong river. In between the aforementioned high and low gravity zones and in the east end and the north end of the survey area, gravity contours run densely in N-S direction. A low gravity zone in the western part of the survey area is distributed in the west of it for the Bouguer map (ρ-2.6 g/cc). Because gravity gradient of the low gravity zone is gentle in the west side compared to the east side, its position of the third order polynomial map is in the west of the Bouguer map.

(5) Gravity distribution by third order polynomial

The highest value of isogravity contours is +2.0 mgals, while the lowest value is -2.0 mgals. The gravity distribution is divided into units of 3 km in diameter.

In the area where basalts are distributed in the east of the Ban Mae Khu Ha fault, there is an anomaly near Huai Mae Khu Ha extending in NW-SE direction. Also in the area south of high gravity the EGAT CAMP and around Ban Mae Pa Khang, there is an anomaly extending in N-S direction.

There are high gravity anomalies extending in NW-SE direction around Ban Kat Khi Lek along the northern extension of the Huai Pong fault and in the east of Doi Luang, where sandstone of the Mae Tha Formation is distributed.

Low gravity anomalies are distributed around Ban Mae Khu Ha, around Ban Pang Riap and northwest thereof along the Huai Ang River and around Wat Hua Fai.

(6) Profiles of underground structure

The subject profiles include iso-gravity profiles, filter profiles, underground structure profiles and geological profiles.

The isogravity profile has been prepared by plotting the results of the two dimensional simulation on the isogravity profile with correction density of ρ = 2.6 g/cm^3 (Bouguer anomaly).

The filter profile expresses the results of third order polynomial residual gravity and spectrum analysis (deep gravimetric component).

The underground structure profile expresses the structural model from the results of simulation.

The geological structure profile expresses geological structure estimated by adding geological information on the surface to the above mentioned results of analysis.

The density structure obtained by the simulation is divided, common to the respective profiles, into the high density mass (ρ = 2.80 g/cm^3), the low density mass (ρ = 2.50 g/cm^3, 2.60 g/cm^3) and the medium density mass (ρ = 2.7 g/cm^3).

The high gravity anomaly in the eastside of the center of the profile is elucidated by the existence of the high density mass (ρ = 2.80 g/cm^3), which is in contact vertically with the low density masses (ρ = 2.60 g/cm^3).

Although the gravity values increase in the western end of the respective profiles, the density model was prepared with homogeneous density of ρ = 2.60 g/cm^3, as the information was not sufficient for density calculation.

The low gravity anomaly in the western part of the profiles can be elucidated by the existence of the low density mass (ρ = 2.60 g/cm^3 and 2.49 g/cm^3). In the area with steep gravity gradient in the central part the profiles, shape of the medium density mass (ρ = 2.70 ~ 2.64 g/cm^3) obtained by the interpretation is different in each profile. It is assumed from the interpretation, in the A-A′ profile and in the B-B′ Profile, that a large volume of the medium density mass is present from the gentle gravity gradient, while a small volume of the medium density mass is expected in the C-C′ profile viewing from its steepest gravity gradient. Correspondence of the density mass to the geological beds in interred to be as shown in the Table 1.2-3.

Table 1.2-3 Correspondence of Density Mass to Geology

Profile / Density mass	A-A'	B-B'	C-C'
ρ = 2.8	Upper part of the Kiu Lom formation	Upper part of the Kiu Lom formation	Upper part of the Kiu Lom formation
ρ = 2.7	Middle to lower part of the Kiu Lom formation		
ρ = 2.66		Middle to lower part of the Kiu Lomformation	
ρ = 2.6 (eastside)	Kiu Lom formation (shale)	Lower part of the Kiu Lom formation (shale)	Lower part of the Kiu Lom formation (sandstone)
ρ = 2.6 (westside)	Middle to lower part of the Kiu Lom formation Mae Tha formation (sandstone)	Middle to lower part of the Kiu Lom formation Mae Tha formation (sandstone)	Middle to lower part of the Kiu Lom formation Mae Tha formation (sandstone)
ρ = 2.49	Lower part of the Kiu Lom formation (chert)	Lower part of the Kiu Lom formation (chert)	
ρ = 2.64			Lower part of the Kiu Lom formation (chert)

As for the isogravity profile, simulation was repeated to seek the most appropriate values by varying shapes and densities of density masses, after an initial model was prepared from the geological profile and the results of density measurement. The isogravity profile was drawn with the most appropriate values thus obtained. Therefore, the final isogravity profile conforms to the geological profile.

1.2.3 Gravity Anomaly and Underground Structure

The underground structure in the survey area is divided in terms of the gravity distribution into the following four blocks of [I], [II], [III] and [IV], by the boundary of large scaled faults or tectonic lines.

[I] block ; the area east of the Huai Mae Koen fault
[II] block ; the area from the Huai Mae Koen fault to the area where limestone bed in the middle part of the Kiu Lom Formation is distributed.
[III] block ; the area from the above limestone bed to the Huai Pong fault
[IV] block ; the area west of the Huai Pong fault and the Doi Luang fault

In the [I] block, shale of the Kiu Lom Formation and sandstone of the Mae Tha Formation are widely distributed. This block is represented by low gravity anomaly caused by the difference of the density of the above rocks from that of the basaltic rocks which are distributed in the west of this block. Dense distribution of isogravity contours found near the Huai Mae Koen fault implies that the fault composes the boundary of different density masses. From the profile analysis, it is estimated that the Huai Mae Koen fault is vertical.

In the [II] block, basaltic rocks belonging to the upper part of the Kiu Lom Formation are distributed. It is thought that variation of densities in the basaltic rocks is small, as interval of isogravity contours is moderate. Also, from the profile analysis, thickness of the beds is estimated to be large. The density of the basaltic rocks, ρ – 2.93 g/cm^3, is the highest of the rocks found in the survey area and the high gravity anomaly extending in N-S direction is caused by the basaltic rooks.

In this area, there are the Huai Wai fault, the Huai Mae Khu Ha fault and other faults crossing the former two. However, except for the southern part of the Huai Mae Khu Ha fault, these faults have no influence on the gravity distribution. The boundary with the [III] block is formed by the Huai Mae Khu Ha fault in the southern half of the block, while in the northern half it is represented by a fault oblique to the Huai Mae Khu Ha fault. This oblique fault is observed to extend from near the point of the geothermal exploration well GTE-3 to around Ban Pan Riap Rua, in NW-SE direction. The Huai Mae Khu Ha fault is almost vertical while this oblique fault is estimated to dip to the east from the results of the profile analysis.

The [III] block is located in the west side of the [II] blook, extending as far to the Doi Luang fault, and is characterized by low gravity zone. This [III] block is further divided into blocks of [III-1], [III-2] and [III-3], from east to west, by the Ban Mae Khu Ha fault and the Huai Pong fault. In the [III-1] area, basaltic rocks are distributed on the surface, as is seen in the [II] block, but gravity value tends to be lower gradually toward the west. By the profile analysis, density of the [III-1] area is ρ = 2.66 ~ 2.70 g/cm^3, which is lower than that of the [II] block of ρ = 2.80 g/cm^3.

In the [III-2] area located in the west side of the Ban Mae Khu Ha fault, sedimentary rocks such as sandstone, shale and chert are distributed. Densities of these rocks are the lowest in the survey area, and it is from the difference of densities of rocks distributed in the [II] blook and in the [IV] block that a low gravity anomaly appears in the area.

By the trend map, further lower gravity anomaly is found in the low gravity zone of the [III] block, and existence of a fault of WNW-ESE trend is estimated there. This lower gravity anomaly extends in an area of 1.5 km by 2 km from near GTE-2 to the area where basalts are distributed in the [III-1] area.

The [III-3] area occupies an area between the Huai Pong fault and the Doi Luang fault comprises density boundary rather more clearly than the Huai Pong fault. In this [III-2] area, sandstone of the Mae Tha Formation is distributed.

The [IV] block contacts with the [III] blook, bounded by the Huai Pong fault in the northern part and by the Doi Luang fault in the south. Sandstone in the [IV] block belonging to the Mae Tha Formation has a little higher density than that of sedimentary rocks of the Kiu Lom Formation, and it is thought that the [IV] block has higher gravity anomaly compared to the [III] block. The Doi Luang fault in the southern part comprises a density boundary. The higher gravity

anomaly relative to the [III] area is in the [IV] block in the west of this fault. From the gravity distribution, step-like faults are thought to exist here.

1.3 Mganetic Survey

1.3.1 Generalization

(1) Magnetic measurement

Two portable proton magnetometers, G-806 and G-846 manufactured by Geometric Inc., were used for magnetic survey with one data recorder and one magnetic susceptibility meter (Table 1.3-1).

Table 1.3-1 Specification of Magnetometer

Type	Maker	Precision
Proton magnetometer Model G-806	GEOMETRICS	Sensitivity 1 gamma
Proton magnetometer Model G-846	GEOMETRICS	Sensitivity 1 gamma
Analogue recorder Model ERP-100A	TOA DEMPA	Sensitivity 1 mV/7.5 cm
Susceptibility magnetometer Model 3101	BISON INSTRUMENT	$1 \times 10^{-5} \sim 1 \times 10^{-1}$ CGS/CC

(2) Base station and diurnal variation measurement

In order to reduce diurnal variation of the earth magnetic field from the collected data, the earth magnetic field was continuously recorded at the base station located in a hut of the EGAT CAMP. Amplitude of diurnal variation of the earth magnetic field during the survey period is about 50 and no magnetic storm was recorded. The example of diurnal variation is shown in Fig. 1.3-1. The magnetic value at the base station was set to 43,556γ.

(3) Magnetic station and measurement method

At the center of the survey area, magnetic field was measured at every 100 m to 200 m along survey lines cut by the EGAT crew. In the surrounding area, it was measured at every 200 m to 500 m along roads and paths. Location of the stations was decided by the survey stakes along the survey lines and by a pocket compass and a chain along roads and paths. All the stations were marked on the 1/10,000 maps. Artificial magnetic noise was very small in the survey area, but five readings were taken at every station and a magnetic value for each station was determined as an average value of the five readings.

(4) Magnetic susceptibility measurement

Magnetic susceptibility was measured in situ at nine outcrops (Table 1.3-2). Because there are not so many outcrops free of weathering, magnetic susceptibility were measured on 84 rook samples including boring cores (Fig. 1.3-2 and Table 1.3-3).

Table 1.3-2 In Situ Measurement of Susceptibility

No.	Rock	Value
S-1	limestone	2×10^{-6}
S-4 68	sandstone	tr
S-5-1 50	chert	2.5×10^{-6}
S-6 14	tuff breccia	tr
S-7-1 26	andesite	3.2×10^{-6}
S-7-2 4	tuff	13×10^{-6}
S-7-3 15	tuff	2.4×10^{-6}
S-9	chert	13×10^{-6}
G-24 47	sandstone, chert	5×10^{-6}

(5) Reduction of diurnal variation

The magnetic value at the base station was set to 43,556γ. A magnetic value at a station (Rs) is calculated as follows;

$$\Delta Rt = 43.557 - Rbt$$

$$Rs = Rst + \Delta t$$

$$Rst + (43,556 - Rbt)$$

where Rbt: the magnetic reading of the base station at the time of the measurement,

Rst: the magnetic reading at the station under consideration

Rt: value of diurnal correction.

(6) Compilation of magnetic map

A total magnetic intensity map, a total magnetic variation map and an upward continuation map were drawn by a computer with magnetic values and locations of all stations.

(7) Spectrum analysis

The total magnetic intensity map and the total magnetic variation map contain waves length from anomalous bodies of different sizes and depths. Shallow structures and deep structures of magnetic bodies can be separated by spectrum analysis (Fig. 1.3-4).

Magnetic structures in the survey area can generally be separated to regional component (HR) of average depth of 760 m and a near surface component (HN) of average depth of 65 m. As a result, a deep magnetic component map and a shallow magnetic component map were drawn.

(8) Model calculation

Magnetic response of a magnetic body depends on three magnetic elements (magnetic intensity, declination, and inclination) of the survey area. It is important to clarify the characteristics of these for the survey area. In this report, three dimensional calculations of magnetic response from a prism model and two dimensional calculations of magnetic response from a dyke model and a fault model are shown in Figures 1.3-5, 1.3-6, and 1.3-7 with different declinations and inclinations.

(9) Two dimensional analysis

Two dimensional analyses were carried out along three sections shown in the magnetic intensity map. An initial structural model was inferred by considering geological information, rock susceptibility measurements, and model studies. A computer calculated magnetic response of an initial structural model. When a calculated magnetic response did not match with the collected data in the survey area, a structural model (location, shape or susceptibility) was automatically modified by computer. This process was repeated until the best fitting structural model was given by the computer. Usually, only one execution of this process would not give an acceptable structural model. Therefore, the individual performing analysis made several initial structural models for each section and on this basis the most appropriate structural model for each section was determined (Fig. 1.3-8).

1.3.2 Results of Survey

(1) Analytical plan and profiles

The following plans and profiles were drawn up from the results of the analysis.

Total magnetic intensity (Fig. 1.3-9)
Total magnetic anomaly (Fig. 1.3-10)
Upward continuation
Deep magnetic oomponent (Fig. 1.3-11)
Shallow magnetic component
Underground structure profile (A-A') (Fig. 1.3-12)
Underground structure profile (B-B') (Fig. 1.3-12)
Underground structure profile (C-C') (Fig. 1.3-12)
Underground structure (Fig. 1.3-13)

(2) Results of susceptibility measurement

From the results of the susceptibility measurement, the following items have been clarified.

① Susceptibility of the basaltic rocks ranges as widely as $10^{-4} \sim {}^{-6}$ cgcemu.
② Values of susceptibility are scattered over a wide range, as a whole. Variation of susceptibility is fairly wide even in the same rock type.
③ Susceptibility of the sedimentary rocks such as shale, sandstone and limestone is mostly less than 10^{-5} cgsemu.
④ Susceptibility of granite is as low as 10^{-5} cgsemu.
⑤ Basaltic rocks belonging to the upper part of the Kiu Lom Formation have high susceptibility among the rocks distributed in this surveyed area.

(3) Outline of magnetic intensity distribution

Forms of iso-magnetic contours of the magnetic anomaly map are almost the same as those of the magnetic intensity map.

Magnetic variation on the magnetic intensity map is from a high value of +112.5 (+43,536) gamma to a low of −184.6 (+43,536) gamma, while on the magnetic anomaly map the highest

value is +113 (43,536) gamma and the lowest value is -175 (+43,536) gamma, taking 0 as the base.

Positive and negative anomalies are expressed as small, closed iso-magnetic contours, which are widely distributed in the entire survey area. The individual areas occupied by such closed circles are as small as 200 to 800 meters in length along their major axis. The closed iso-magnetic contours are found predominantly in the area where basaltic rocks are distributed, but not all correspond to the distribution of the basaltic rocks. It can be said that they are distributed along the Ban Mae Khu Ha fault and along the Huai Mae Khuha fault as well as in the area surrounded by these faults. The closed iso-magnetic contours are also found along the Hual Wai fault. Negative anomalies which have rather large area are distributed along the above faults or along the faults oblique to the above faults. In the area where shale, chert and sandstone are distributed, almost no magnetic anomaly has been found.

As for distribution of negative anomalies, an anomaly surrounded by an iso-magnetic contour of 10 gamma of approximately 1,000 m long along its major axis is found about 800m west of the EGAT CAMP, about 700m north of the site of the geothermal exploration well GTE-4, and another negative anomaly 1,500 m long along its major axis is found at the upstream of the Huai Ko Pong river.

(4) Outline of deep magnetic component map

The deep magnetic component map has the following characteristics compared to the magnetic map.

Variation of the magnetic anomalies is from a high of 47 gamma to a low of -55 gamma. The individual areas expressed by the closed iso-magnetic canters are rather wide, though number of the anomalies is smaller.

Locations of positive anomalies and negative ones on this map are almost coincident with those on the magnetic anomaly map. The anomalies are distributed along the Huai Mae Hhu Ha fault, the Ban Mae Hhu Ha fault, the Huai Wai fault and the Hual Mae Koen fault.

A negative magnetic anomaly whose major axis is approximately 1,000 meters is distributed about 800 m west of the EGAT CAMP and about 700 m north of the geothermal exploration well of GTE-4.

(5) Underground structure profiles

The three profiles (A-A′, B-B′, C-C′) have been analyzed. They are the same as the gravity profiles.

Along these profiles, the magnetic anomaly profiles, the filtered profiles and the underground structure profiles have been displayed.

Filtered profiles express the results of spectrum analysis (deep component and shallow component) and the upward continuation.

Underground structure profiles expresses the structure model obtained by the results of the simulation.

The magnetic bodies analyzed are distributed in dyke shape in shallow to deep ground, seated in the Kiu Lom Formation.

The calculated susceptibility is $3 \sim 37 \times 10^{-4}$ cgsemu, which is in the range of susceptibility of

the basaltic rocks in the Kiu Lom Formation.

1.3.3 Magnetic Anomaly and Underground Structure

Viewing from the analysis results of the magnetic survey, the underground structure in this survey area is divided into three blocks.

[I] block ; the area east of the Huai Mae Khu Ha fault and the Huai Wai fault
[II] block ; the area from the Huai Mae Khu Ha fault and the Huai Wai fault to the Ban Mae Khu Ha fault
[III] block ; the area west of the Ban Mae Khu Ha fault

In the [I] block, the Kiu Lom Formation is widely distributed. The number of the magnetic bodies analysed in this block is comparatively small and their distribution is irregular.

In the [II] block, the upper part of the Kiu Lom Formation is distributed in the eastern part, bordered by the limestone bed of the middle part of the Kiu Lom Formation, while the middle to lower part of the Kiu Lom Formation is distributed in the western part of the limestone bed. There are faults of N-S trend such as the Huai Wai fault, the Huai Mae Khu Ha fault and the Ban Mae Khu Ha fault, in addition to the other faults crossing the above faults in the NW-SE direction. The magnetic bodies analysed are numerous, and most of them are distributed along the above-stated faults. Other magnetic bodies than those found along the faults, located in a row in the north to south direction near Ban Mae Khu Ha.

The [III] block is the area where the sedimentary rocks of the middle to lower part of the Kiu Lom Formation are distributed. By the results of the susceptibility measurement, susceptibility values of the sedimentary rocks are small, and no marked magnetic body is recognized in this block. In the area east of the Huai Mae Koen fault comprising the eastern part of the survey area, magnetic structure is similar to the above.

It has been clarified that the magnetic bodies in the survey area are distributed, as aforementioned, in the area where the middle part of the Kiu Lom Formation is found, and that most of them are found in the area south of the Huai Wai fault, along the Huai Mae Khu Ha fault and along the Ban Mae Khu Ha fault. As there is an intimate relation between the distribution of magnetic bodies and that of the faults, it is possible that some subsurface faults would exist in the vicinity of the area around Ban Mae Khu Ha where magnetic bodies are distributed.

By the results of measurement of susceptibility, susceptibility of the upper part of the Kiu Lom Formation is higher than that of the other formations, and the values range widely over. However, no relation has been recognized between distribution of the magnetic bodies, and distribution and shape of the upper part of the Kiu Lom Formation. However, distribution of the magnetic bodies is thought to be related intimately with locations of faults.

As a result of the presence of these magnetic bodies, certain layers in which magnetic minerals are concentrated, certain parts in basaltic rocks where magnetism is specially strong and certain high magnetic intrusive rocks are thought to exist in this area. In case that magnetic bodies are characterized by the former two features, distribution of the magnetic bodies would correspond to the strike and distribution of certain formations. However, distribution of magnetic bodies corres-

ponds to location of faults. Therefore magnetic bodies are thought to represent the existence of some magnetic intrusive rocks along faults, or to represent change of geological formations bounded by the faults.

1.4 Seismic Survey

1.4.1 Generalization

The seismic survey was aimed at sounding the ground by the seismic reflection method to explore bedding planes, faults and other geological structures in order to identity those structures, such as fracture zones, which control the existence of geothermal fluid.

Seismic survey is a method to sound geological structures by generating artificial earthquakes in the shallow layer of the earth and measuring elastic waves from the seismic sources. The seismic reflection method employs elastic waves reflected by bedding planes which have different elastic properties (reflection coefficiency).

In general, reflected waves in an area of complicated geological structure, such as a geothermal field, are expected to be weak. To meet such circumstances, six-fold stacking with a common reflector was employed in this exploration.

The number of survey lines used in this exploration was five (Lines A, B, C, D and E) with a total length of 14,225 m. A total of 315 shot holes were made.

1.4.2 Field Survey

(1) For the seismic reflection survey, five survey lines A, B, C, D and E were cut so that a prospective area along the Huai Pong fault was covered by the lines. The details of the survey lines are shown in Fig. 1.4-1 and Table 1.4-1.

Table 1.4-1 Specification of Exploration Lines

Line Name	Line Length (m)	No. of Spread	Station		No.		No. of Spread
			No.	Interval (m)	No.	Interval (m)	
A	5,475	99	220	25	105	50	NW
B	2,025	30	82	25	36	50	NE
C	2,025	30	82	25	36	50	NE
D	2,025	30	82	25	36	50	NE
E	2,675	43	108	25	49	50	NE
Total	14,225	232	574	–	262	–	

Line A starts at the northwestern mountains of the survey area, crosses several likely faults, and reaches Ban Mai community in the southeastern part of the area, with a total length of about 6.5 km.

Lines B, C and D cross line A almost perpendicularly and run in the direction of NE-SW for as long as about 2 km each, from the piedmont of the western mountains of the survey area to the plain in the east part of the area.

Line E was laid in the southernmost part of the survey area, is 2.7 km long, and generally runs over hilly relief of low elevation.

(2) Shot hole drilling

Shot holes were drilled 10 m deep using 6 to 10 portable rotary drills, and were completed by insertion of vinyl chloride plastic pipes of 76 mm in diameter for maintenance.

(3) Blasting and observation

Explosive charges of between 10.0 kg to 12.5 kg was inserted in the bottom of each hole drilled along the survey lines. After filling the hole with water, blasting was performed.

Seismic waves were recorded with a 24-component seismic exploration system of magnetic tape recording (PT 100 + MR 20R-6B) manufactured by SIE (USA), and 36 groups of geophones (EV-15, natural frequency 20 cps) manufactured by ETL (USA). At each receiving station, six geophones were placed in a group (arrayed linearly along the survey line at an interval of 2 m). Horizontal six-fold stacking, mainly with end blasting, was employed in order to improve signal:-noise ratio of reflected waves, and also to enhance resolution for better identification of geological structures (Fig. 1.4-2,3).

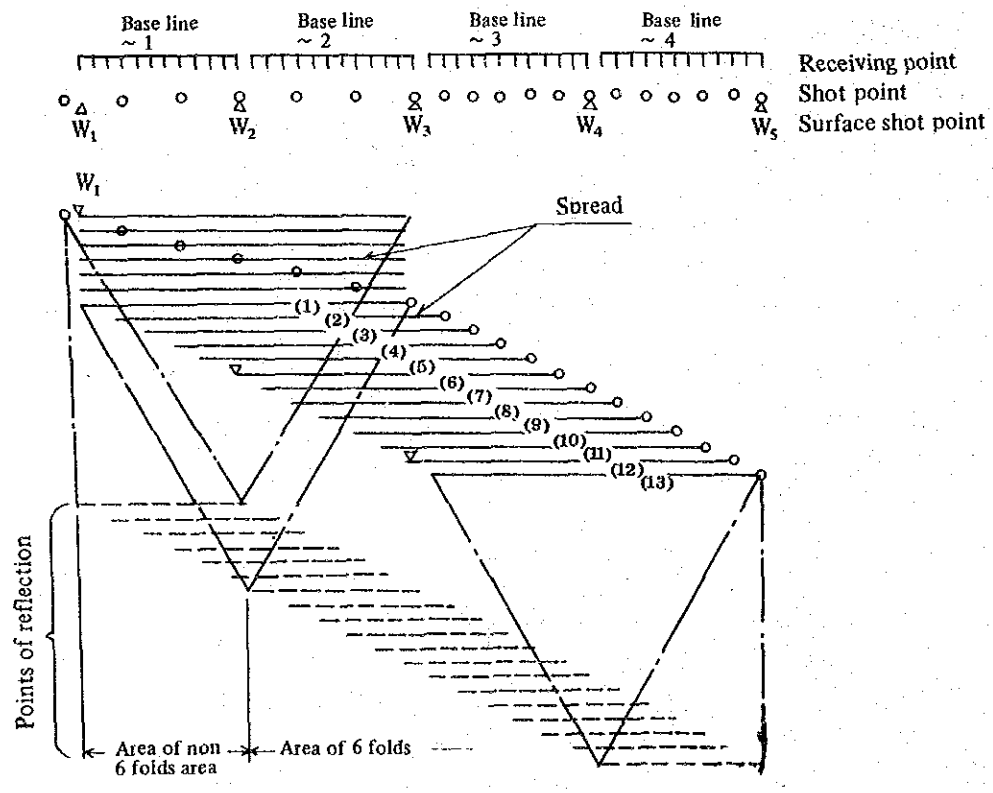

Fig. 1.4-3 Process of Measurement by Common Reflection Point Horizontal Stack Method (6 fold)

1.4.3 Method of Analysis Field Data

(1) Method of analysis field data

1) Analysis by the seismic refraction method

The seismic refraction analysis method was utilized for calculation of static corrections. A shallow layer down to the datum plane (for this survey 300 m above sea level), was subjected to weathering correction and datum correction. The extent of the corrections was obtained from expressions for calculating a double layer structure.

Besides such interpretation for static corrections, a calculation for triple layer structure was done also by the refraction method by means of first break travel time curves, in order to obtain the distribution of a shallow velocity layer.

2) Analysis of deep layer structure by the seismic reflection method

Stacking is a method to emphatically show waves reflected on a given reflecting point, by preparing a single reflection record from several records at various distances from the epicenter after correcting their difference in travel time. When this method is applied, irregular noises are attenuated by their mutual interventions because, unlike signals, individual noises have different time lags. This improves the signal: noise ratio of the reflection waves.

To the stacked records obtained in this way, the analysis methods of obtained frequency distribution, signal: noise ratio distribution, diffraction sourse distribution, etc. were applied and resultant data employed as material for interpretation of the geological structure (Table 1.4-2).

Table 1.4-2 Outline of Wave Analysis

Type of analysis	Result	Application	Method
Wave analysis trace type (LH group)	Frequency-Time curve Amplitude-Time curve Frequency-Fourier curve Amplitude-Frequency curve Amplitude-Fourier curve	comprehension of wave properties	Digital analysis by electronic computer
	Fourier analysis or Power analysis	as above	Digital analysis by electronic computer
Wave analysis profile type (each survey line)	Frequency distribution S-N ratio distribution	judgement of geothermal source and alteration zone	Digital analysis by electronic computer
Side reflection analysis (each survey line)	Side reflection analysis map Side reflection distribution map	judgement of boundaries of layers and formations and judgement of structure lines	Reading with eyes
Diffraction source analysis profile type (each survey line)	Diffraction source distribution map Diffraction compilation map	as above	as above

(2) Method of additional analysis

Based on the data obtained from seismic exploration, the following additional analyses were conducted to prepare cross sections for the survey lines A, B and C.

1) Instantaneous frequency analysis cross sections

An instantaneous frequency cross section illustrates, in color, phase modulation ratio:

$$(W(t) = -\frac{d\theta(t)}{dt})$$

between the real and imaginary part (R(t) and I(t), respectively) of the actual reflection wave data which have been transformed by Hilbert transformation.

In these cross sections, the more warm and white the color is, the more dominant the lower frequency zone is; and the more cool the color is, the more prevailing the higher frequency zone is (Fig. 1.4-4,5 and 6).

2) Real trace amplitude cross section

A real trace amplitude coross section illustrates in color the amplitudes (Rm) of individual reflected waves after wavelet processing, with the intensity of these amplitudes being reflected by color brightness for classification (Fig. 1.4-7,8 and 9).

(3) Method of re-interpretation of seismic exploration results

The main object of the preceding seismic exploration interpretation was to identify direct correspondence of the processed cross sections to geological horizons. However, the seismic exploration (reflection method) is designed, by nature, to be basically applicable to a stratified structure. In the present survey area for which a complicated geological environment has been indicated by drilling in well GTE-7, it seemed unreasonable that the processed cross sections should be used as such for geological interpretation.

Because of the need to review these seismic exploration results in view of such geological environment, results were reinterpreted with special stress on identification of fracture systems. This work dealt only with the survey lines A, B, and C, and was mainly devoted to extracting vertical discontinuities and reflectors from the typical processed cross section (i.e., time cross sections and depth cross sections).

During this work, reference was also made to those cross sections of physical property interpretation, which had been obtained by the additional interpretation mentioned above. They served as criteria for qualitative determination of vertical discontinuities and reflectors, and for identifying fracture systems.

Components of this work are outlined, as follows.

1) Identification of reflectors

Clear and continual reflectors were identified from the processed cross sections for each survey line. Basically, time cross sections and depth cross section were utilized. In addition, real trace amplitude cross sections were referred to.

The time depth sections, both before and after migration, were compared and examined. The pre-migration cross sections were adopted because in the end they were better in quality and more suitable for interpretation.

In these processed cross sections, however, a large number of multi-reflected waves or diffracted waves were understood to be mixed with simply reflected waves, so that the cross

sections were deemed unsuitable for direct correlation with actual geological structures. For this reason, all reflected waves extracted from each cross section were illustrated in ranked fashion according to clearness and continuity. The identification and ranking of the reflected waves were based on time cross sections, and real trace amplitude cross sections were used for reference.

In the final illustration, depth was taken as the ordinate. The ranking of reflected waves on the depth ordinate was made by comparing the reflected waves obtained from the time cross section with those from the depth cross section.

The reflectors which are ranked high on the illustration are more likely to correspond to formation borders, or to high contract in physical properties, of rock facies, while those which are ranked low may be diffracted or multi reflected waves. In any case, such a ranked illustration of a large number of reflected waves is expected to permit comparison of the reflected wave cross sections to the results of other categories of the survey, and to serve to improve the overall geological interpretation.

2) Discontinuity of reflectory in the vertical direction

When an exploration line is crossed by a fault or fracture zone, the zone is often represented directly be vertical discontinuity of a reflector on a processed cross section.

Yet, there seemed considerable risk that such vertical discontinuities on a processed cross section may result from problems in processing the complicated geological structures, or from influences of multi-reflected waves and diffracted waves. Direct relating of such vertical continuities to the existence of a fault or fracture zone would be precarious.

Tanking this into account, the discontinuities of the extracted reflected waves were illustrated in ranked fashion according to the clearness of each discontinuity.

A time cross section was used as the base from which the vertical discontinuities were extracted and by which discontinuities were ranked. Real trace amplitude cross sections and instantaneous frequency cross sections were also employed for reference.

In the final illustration, depth was taken as the ordinate, and the ranked discontinuities on the depth coordinate were illustrated in ranked fashion by the same procedure as for the reflector ranking.

While those discontinuities which are ranked high in the illustrations are likely to correspond to faults or fracture zones, those which are ranked low may result from problems of processing, such as velocity analysis, and also from the influence of diffracted waves and multi-reflected waves. Nevertheless, as in the case of ranking of the reflected waves, illustration in a ranked manner of all discontinuities that may possibly represent geological discontinuities, and comparison of this cross section with the results of the other categories of the survey can serve to improve the geological interpretation.

3) Extraction of low-frequency-band-dominant zones

When reflected waves have passed through a fault, fracture, or other rock body having large internal friction, such reflected waves show a dominant tendency to have lower frequency level.

Giving attention to this tendency, low-frequency-band-dominant zones were extracted from each instantaneous frequency cross section, and such zones were compared with other processed cross sections and the results of the other categories of the survey. The instantane-

ous frequency herein means a moderation ratio:

$$(W(t) = -\frac{d\theta(t)}{dt})$$

of the phase value $(\theta(t))$ of reflected waves. It is therefore dependent also on other geological conditions, and this inhibits the direct relating of the low frequency zone to faults and fracture zones. Notwithstanding this, comparison of the extracted low frequency zones with other processed cross sections and the results of other categories of the survey will help delineating the locations of faults and fracture zones.

1.4.4 Results of Analysis

In the interpretation work after the second phase survey, time cross sections and depth cross sections were prepared by means of depth calculation, stacking, wave form analysis, and other techniques, and a geological interpretation was given to these cross sections. However, a seismic survey of reflection method is designed, by nature, for a stratified geological structure. In an area having such complicated geological structure as the subject survey area, a processed cross section of seismic exploration cannot normally be applicable directly to geological interpretation without further processing. For this reason, additional analyses were performed to obtain vertical discontinuities of reflectors, and instantaneous frequency cross sections were also determined. Principal analysis results are as follows.

(1) Structural cross sections of seismic exploration

Both the extracted reflectors and the vertical discontinuities of such reflectors are illustrated together on all structural cross sections for individual exploration lines of the seismic exploration (Fig. 1.4-10 and Fig.1.4-11), as outlined in the following.

1) Survey Line A

In this processed cross section, a large number of multi reflected waves are understood to be contained, and no true reflectors can readily be identified. However, reflected waves are relatively continual, and several distinot reflected waves can be identified. These facts indicate that the near flatness of the plane on which this survey line lies has eliminated most of problems for static correction. In this sense, this cross section can be assessed as fairly good.

It is remarkable that reflected waves around a range from station 40 to station 120 are particularly clear at a depth of -2,000 m, and that they are highly likely to correspond to actual reflectors.

The vertical discontinuities of reflectors, which can be identified in large number, seem to be mostly resulting from the influence of diffracted waves and multi-reflected waves, as well as from problems in processing. They are not clear enough to permit their being directly correlated to any fault or fracture zone.

A relative exception are the rather clear vertical discontinuities in the vicinities of station 90, which correspond well to the low velocity zone (2,900 m/s) in the shallow layer identified in the refraction method interpretation for static correction use.

2) Survey line B

Like line A, a large number of multi-reflected waves are contained in the cross section of

line B, and quality level of this cross section is approximately equal to that of line A cross section.

However, clearer and more continual reflected waves than those of line A can be observed around a range from station 25 to station 60 at a depth of -2,000 m, and they are more likely than in the case of line A to correspond to an actual reflector.

Another group of reflected waves, relatively clear and continual, is identified in the vicinity of -4,000 m to -4,500 m in depth, but they are likely to be double - reflected waves which have rebounded off the reflector mentioned above.

It is interesting that a large number of reflected waves tend to be titled in the direction of greater serial number side of the stations (viz. northeast).

Among the vertical discontinuities of reflected waves, a relatively clear discontinuity can be observed in the vicinity of station 40.

3) Survey line C

Like lines A and B, a large number of multi - reflected waves are contained in the cross section of line C, and the qualitative level of the waves are also approximately equal to those of lines A and B.

Relatively clear reflected waves are observed in a range from station 10 to station 40 at about -1,600 m to -2,300 m in depth, and also in a range from station 50 to station 75 at about -2,300 m to -2,500 m in depth.

Like line B, it is interesting that a large part of the reflecting planes tend to tilt toward the northeast.

Relatively clear vertical discontinuities of reflected waves are observed in the vicinities of station 30 and station 60.

(2) Extraction of low-frequency-band-dominant zones, and comparison with structural cross sections

Comparison of the instantaneous frequency cross sections with the structural cross sections is discussed as follows.

1) Survey line A

In the instantaneous frequency cross section of line A,relatively clear indications of low-frequency-band-dominant zones are identified. One is in a range from station 5 to station 40, another in a range from station 80 to station 110, and yet another in a range from station 130 to station 150. Each of these zones are distributed almost continually, extending from the shallow to depth ground. Another low-frequency-band-dominant zone, somewhat less clear, can be observed around a range from station 45 to station 70 at about -500 m to -3,500 m in depth.

In the structural cross section, three discontinuities, including one clear vertical discontinuity, are identified in a zone corresponding to the said low frequency zone that ranges from station 80 to station 110. It seems highly likely that fracture systems are developed here. In addition, a clear vertical discontinuity is observed at each of two locations which correspond to low frequency zones in a range from station 5 to station 40, and in a range from station 130 to station 150. It is highly likely that fracture systems are developed at these locations.

Although not clear, three discontinuities are observed in the low frequency are in a range

from station 45 to station 70.

It is to be noted that, although almost all the deeper ground (about -6,000 m or more in depth) tend to be low-frequency-band-dominant. This seems to be a result of the attention of high frequency components in waves.

2) Survey line B

A clear low-frequency-band-dominant zone is identified in a range from station 1 to station 25, extending almost continually from shallow to deep ground. Another low-frequency-band-dominant zone is observed although not clearly defined, in a range from station 50 to station 80 at about -500 m to -4,000 m in depth.

In the structural cross section, no clear vertical discontinuity can be identified at a location corresponding to the said low frequency zone ranging from station 1 to station 25. No clear vertical discontinuity is observed at the said location of the low frequency zone ranging from station 50 to station 80, either.

A clear vertical discontinuity is identified around station 40, but this is a part of a relatively high frequency zone, and here, the two cross sections do not correspond well. One conceivable reason is that a discontinuity probably exists, but no fracture zone may have developed to any extent around it.

3) Survey line C

There are two relatively clear low-frequency-band-dominant zones. One is in a range from station 1 to station 15 at about -1,000 m to -4,500 m in depth, and the other is in a range from station 25 to station 45 at about -1,000 m to -5,000 m in depth.

In the structural cross section, a relatively clear discontinuity is observed at each of the two locations mentioned in the preceding paragraph, and this indicates that in these locations fracture systems are likely to be developed. One clear discontinuity is identified in the range from station 60 to station 70, but around this location the low frequency zone is weak.

1.5 Deep Electrical Survey

1.5.1 Generalization

Deep electrical survey was carried out to collect information about the geothermal reservoir through both the magnetotelluric method (MT) and the controlled source audio-frequency magnetotelluric method (CSAMT). Both methods measure ratio of induced magnetio field and electric field to identify resistivity (or conductivity) distribution in the area.

In the MT method, three components of magnetic fields (Hx, Hy, and Hz) and two components of electric fields (Ex and Ey) naturally induced in the earth were measured. In the CSAM method, two components of magnetic field (Hx and Hz) and one component of electric field(Ey) induced by a transmitting loop were measured.

In the second phase survey, MT and CSAMT measurements were done at the same 33 stations.

As a result, apparent resistivity distributions maps of several frequencies were compiled. One-dimensional inversion was carried out at each station. From one-dimensional inversion of all the stations, a total conductance map, a resistivity structure map based on conductive layer surface

structure, an isopack map of the overlaying layer (equi-thickness contour map) and a resistive basement map were compiled. Two-dimensional analysis was carried out across conductive anomalous zones obtained from analysis of resistivity maps to infer location of fractured zones.

The supplementary survey was to pinpoint location of a exploratory well for the third phase survey and to clarify extension of the conductive zone in Ban Mae, southeast of the survey area. It was carried out around the conductive zones found by the second phase survey. In the supplementary survey, MT was measured at 20 stations and CSAMT measurement was carried out to the same 20 stations.

1.5.2 Field Survey

(1) Method of MT Survey

1) Field work procedure

The field work procedure for MTmethod is s follows (Fig. 1.5-1).

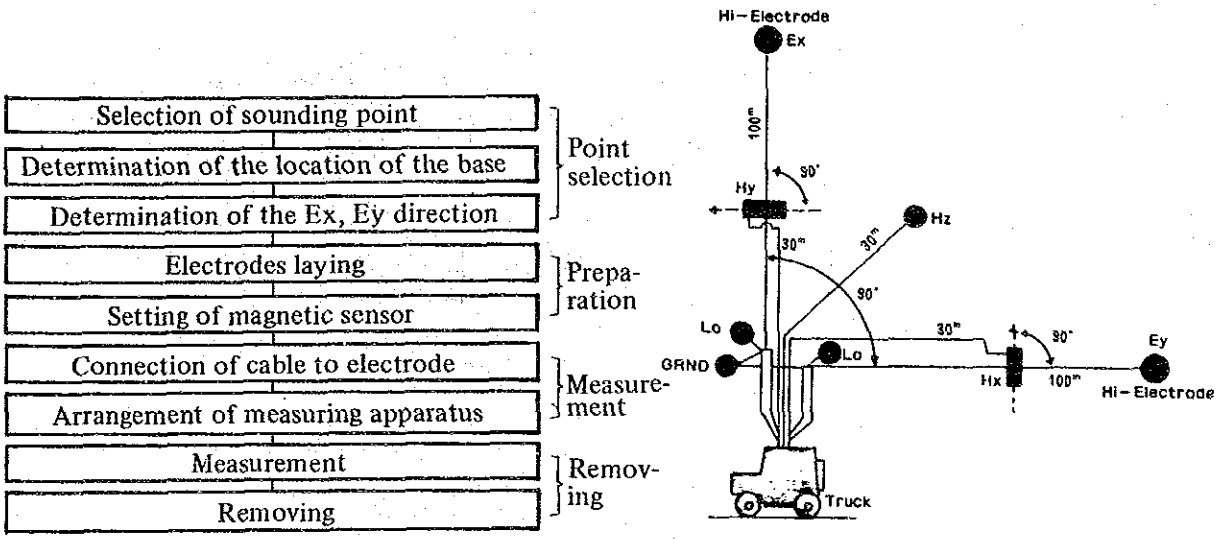

Fig. 1.5-1 Measurement of MT Survey

2) Selection of measuring points

Those spots where field conditions would actually permit measurement were selected at or around the planned measuring point locations. Taking full account of site conditions, a base location was selected so that on this location two survey lines may cross each other perpendicularly. Then two survey lines, 100 m long each, were set, passing a base location.

3) Preparations for measurement

Hx and Hy coils were orientated by compass perpendicular to the Ey line and Ex line, respectively, and horizontally installed by a leveller. The Hz coil was buried about 60 cm deep in the ground, and installed vertically by a leveller.

Each of these coils was protected from direct sun shine and wind by covering it with a wood box or polyethylene bucket, and then piling soil over the box or bucket to prevent its movement.

Cables were connected to electrodes with wire nuts. Each connection point was proteoted from direct sun shine by covering it with a connection box, and then by grass and tree branches.

4) Measurement

Cables were connected to the measuring instruments, and coil impedance and grounding impedance were measured, which next individual cables were connected to the panel and the amplifier adjusted. Cassette tapes were set in a data logger, and after checking incoming signals the data logger was started to record signals.

During measurement, graphic paper sheets were monitored, and whenever noises were observed, cause of noise was sought. With a view to analyze electric and magnetic field with periods 200 seconds, every 25-minute record was separated as a single file of data in the case of a single measurement. At least four files of noise-free record were collected per single meaurement.

5) Instruments

Specifications of the instruments used for the sounding (manufactured by GEMP) are tabulated below Table 1.5-1).

Table 1.5-1 Apparatus for Measurement of MT Survey

Instrument	No.	Specification
Electric field amplifier unit	2	(1 st stage) Input level: 1 μV Maximum gain: 2 x 10 1.00 Hz high-cut filter (2nd stage) Maximum gain: 10 0.33 Hz high-cut filter
Magnetic field amplifier unit	3	Maximum gain: 2 x 10 0.33 Hz high-cut filter
Wave form recorder	1	Full scale: ±5V Chart speed (2-stage variable): 0.085 cm/s & 0.17 cm/s
Data-logger (Double cassette)	1	Full scale: ±5V Sampling rate: 100 ms/1 data, 5 sample multiplexer
Battery	2	12V, 100A
Magnetic sensor (induction coil)	3	115 mm (ϕ) x 1050 mm (L), appr. 10 kg
Accessories	1 set	MT cables, electrodes, tools

(2) Method of CSAMT Survey

1) Measuring process

Electric power generated by a 1-kW generator was transmitted by a transmitter into a

square loop having four sides of about 300 m each to generate an artificial magnetic field. Frequencies of the transmitted current in the second phase survey comprised 9 steps: 280 Hz, 140 Hz, 70 Hz, 35 Hz, 175 Hz, 8.75 Hz, 4.38 Hz, 2.19 Hz and 1.09 Hz. In the supplementary survey, there were 12 steps: 2,240 Hz, 1,120 Hz, 560 Hz, 280 Hz, 140 Hz, 70 Hz, 35 Hz, 17.5 Hz, 8.75 Hz, 4.38 Hz, 2.19 Hz and 1.09 Hz.

Receivers were installed at about 700 m to 1,500 m awa from this loop, and sensors for Hx, Hz and Ey components received signals. Signals received, which were as weak as between 10 σV to 20 σV, were amplified, and screened by both an appropriate band bass filter that fitted the frequency level of the current flowing along the loop, and 50 Hz notch filter. In the end, each averaged value of data was digitized and indicated on a panel for direct reading and recording (Fig. 1.5-2).

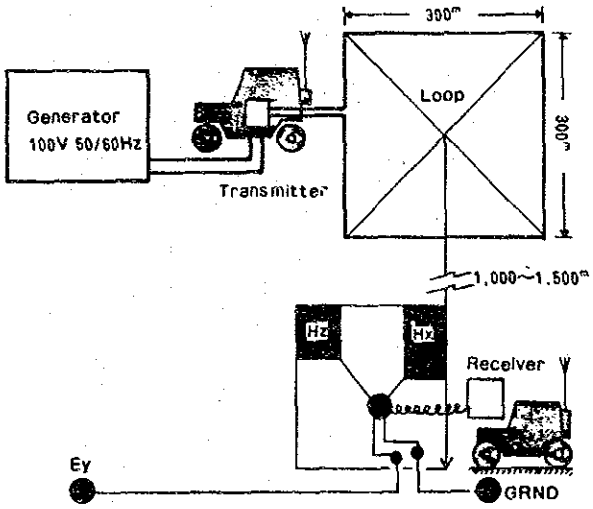

Fig. 1.5-2 Method of Measurement of CSAMT Survey

2) CSAMT measuring instruments

Instruments used for CSAMT survey (manufactured by GEMP) are indicated in the following table.

Table 1.5-2 Apparatus for Measurement of CSAMT Survey

Instrument	No.	Specification
Transmitter	1	Frequencies (Hz): 280, 140, 70, 35, 17.5, 8.75, 4.38, 2.19, 1.09 Power: 1 kW
Receiver	2	Input level: 10 μV Output display: digital in 4 digits Band pass filter and notch filter: 50 Hz/60 Hz
Sensor	1 set	Telluric sensor: 1 Magnetic sensor: 2
[Accessories] Tools Handheld computer for data processing (Used for the supplementary survey) Others		1 set 1 set 1 set

1.5.3 Method of Analysis of Field Data

The collected data were inverted into one-dimensional layered structure models. From the results of one-dimensional inversion, a total conductance map and a resistive basement map were compiled. Two-dimensional analysis was carried out for conductivity anomalies in the above mentioned maps. Flow chart of the interpretation is shown in Fig. 1.5-3.

Apparent resistivity, pa, of CSAMT is calculated as follows:

$\rho a = (K/\mu o f)\,[Ey/Hx]$

where, K : correction factor
μo : magnetic permeability
f : frequency
Ey : electrio field in y direction
Hx : magnetic field in x direction

For MT data, the following values were calculated.

① apparent resistivity vs frequency curve with error bar after coordinates rotated
② apparent resistivity curve calculated from an inverted one-dimensional layered model.
③ rotation angle
④ total conductance
⑤ layered ground model from one-dimensional inversion.

1.5.4 Results of Analysis

(1) Second phase survey

1) Apparent resistivity maps (Figures 1.5-4 and 5)

Apparent resistivity distributions of frequencies (periods), 8.75 Hz, 11 second and 39 second are shown in figures 1.5-4 and 5. Electromagnetic theory indicates that apparent resistivity distribution of lower frequency shows deeper resistivity structure in the ground. On the contrary, the higher trquency (in this case 8.75 Hz) indicates shallow resistivity structure.

The maps show that resistivity in the survey area is fairly high. Low resistivity zones are at a present geothermal manifestations centered at station 2-2 and the southeastern area including stations 2-7, 3-6, and 4-5. The southeastern anomalous area is thought to be very large, but its extent is not clear because the anomalous area is at the edge of the survey area.

2) Total conductance map

A value of total conductance is a sum of conductance over a resistive basement after apparent resistivity curves have been inverted one-dimensionally. Total conductance is calculated as follows:

$$TC = \sum_{i=1}^{n} \frac{hi}{\rho i}$$

where, TC: total conductance (mho)
hi: thickness of a layer (m)
ρi: resistivity of a layer (Ωm)

Total conductance distribution shows resistivity anomaly above the resistive basement (Fig. 1.5-6)

As with the apparent resistivity maps, two areas of anomaly are present on the total conductance map. In general, total conductance values are low and variation is not large. This indicates that resistive layers dominate the survey area.

3) Map of top of conductive layer (shallow and deep)

The maps show the shape of the top of conductive layers after data as inverted for one-dimensional resistivity structure. As there are two conductive layer formations found in the survey area, one shallow and one deep, two conductive layer top maps are presented for the said deep and shallow layers. (Fig. 1.5-7 and 8). The map of the top of the shallow conductive layer exhibits the shallowest point at around survey station 2-2, and depth thereof is 400 m to 0 m above sea level. The depth of portions is mostly above sea level and has no significant undulations.

Pattern of the map of the top of the deep conductive layer is very similar to that of the total conductance map. High conductance area coresponds to anticline of the deep conductive layer top map. Undulations of this map are very steep, from -3,000 m to -9,000 m below sea level. Therefore, the precondition of one dimensional inversion, horizontal does not hold here and interpretation by a computer was carried out in the area.

4) Isopack map of the resistive top layer

This map shows change in thickness of the overlaying layer, from the surface to the deep conductive layer (Fig. 1.5-9). For preparing sub-maps, thickness is divided into the following three classes. ΔH

D1: thickness, ΔH, is under 1,000 m

D2: thickness, ΔH, is between 1,000 m and 3,000 m

D3: thickness, ΔH, is over 3,000 m

5) Electrical basement map

The map shows undulation of the top of the Rb layer and Rc layer, which are referred to as the resistive basement when total conductance is calculated (Fig. 1.5-10).

The pattern of this map is similar to that of the map of the top of the conductive layer. It shows that undulation of the top of the deep conductive layer corresponds to that of the basement.

However, at the centers of the anticline and the sincline, depths of the two maps differ. The difference shows change of thickness of the conductive layer.

(2) Supplementary survey

The supplemenmtary survey revealed resistivity structure of the areas around Nat Pong Hom in the northwest of the survey area and around Wat Hua Fai in the southest of the survey area.

The results of one-dimensional inversion show two important conductive layers. The one is the Ca layer (average resistivity: 3 Ω-m) at shallow depth and the other is the Cb layer (average resistivity: 5 Ω-m) at deeper depth.

Two conductive anomalies are recognized in the total conductance map (Fig. 1.5-11). The one is at the center of the survey area including stations 2-1, 2-2, and 103, and the other is at the southeast of the survey area including stations 3-6, 4-5, 112 and 113. This survey clarified the extension of the southeastern anomaly, which is rather large.

The anticline in the map of the top of the deep conductive layer (Fig. 1.5-12) is where the total conductance anomlay is. Because this anticline coincides with the anticline of the electrical basement, there is thick conductive layer over the convex of the electrical basement causing conductive anomaly.

Two-dimensional analysis was carried out for two sections cutting across a low resistivity zone around Wat Pong Hom in the northwest of the survey area (Fig. 1.5-13 and 14).

The A section connects stations 1-2, 105, 2-2, 106 and 3-2.

The B section connects stations 2-1, 103, 2-2, 109 and 203.

In the figure for the two-dimensional sections, F means a fractured zone where conductivity is very high and extension is small. Resistivity of a fractured zone is assumed to be 1 Ω-m.

As a result of integrated interpretation of the supplementary survey, the following three areas have high potential for geothermal development and it is recommended that exploratory wells be drilled therein.

① Around station 2-2

Station 2-2 is in the central low resistivity anomaly zone including stations 2-1, 2-2 and 103. This anomaly zone extends slightly along the NW-SW axia. Both two-dimensional sections show that station 2-2 is at the center of a conductive layer of great thickness, about 2,000 m. Such a thick conductive layer has high possibility of containing good fractures.

② Around station 4-5

The southeastern anomaly is very large and attractive. Station 4-5 is assumed to be a prospective drilling point. Local geological condition of station 4-5 is similar to that of station 2-2, with high total conductance, a thick conductive layer and location at the axis of the anticline of the electrical basement. Therefore, station 4-5 is recommended as a prospective drilling point.

③ Around station 112

Station 112 is at the north of the eastern conductive anomaly zone with a very thick conductive layer. However, station 12 is relatively isolated.

1.6 Geochemical Survey

Geochemical surveys have been conducted repeatedly by the counterparts in Thailand prior to the starting of this survey program. The results are described briefly as follows.

1.6.1 Chemical Composition of Thermal Water

The thermal water obtained from the San Kampaeng area shows weak alkaline character of pH ca. 8 - 9 and its alkalinity is ca. 300 - 430 (mg/ℓ $CaCO_3$). The chemical composition is a type of Na-HCO_3-SO_4 phase i.e., the major cation is Na^+ and the major anions are HCO_3^- and SO_4^{2-} (Fig. 1.6-1, Table 1.6-1).

The most distinguishing characteristics of the thermal water in this area are that the total amount of the dissolved solid is less than 1,500 mg/ℓ, the chlorine content is less than 80 mg/ℓ, and the SiO_2 is about 120 ~ 150 mg/ℓ. These values are quite small. Judging from these results, there is little possibility that the geothermal fluid is heated by the volcanic gas and/or high

temperature steam direotly from magma.

It is estimated that the surface water has mixed with the deep geothermal water because of the difference of Mg ion content in each source and the seasonal change of Cl ion content in the outpouring hot water (Fig. 1.6-2).

To know the travel time of the geothermal water from the initial recharge of the surface water to the stage of pouring out to the ground surface after being heated deep under ground, the tritium measurement has been applied. The tritium content in the thermal water taken from the San Kampaeng area is found to be 4.5 and 9.0 TU($T/U \times 10^{18}$). In general, it is said that the water with tritium of 3 ~ 20 TU is due to the mixing of high tritium concentration water resulting from atmospheric hydrogen bomb testing during 1952 ~ 1962.

It can be estimated that the thermal water in the San Kampaeng area is as old as about nearly thirty years. However, the thermal water pouring out to the surface is considered to be mixed with young surface water. Therefore, taking this mixing effect into consideration, it is estimated that the age of the geothermal water pouring out is more than 30 years as this is the time that would be required for such water to circulate deep underground.

Table 1.6-1 Chemical Compositions of the Hot Spring Water in the San Kampaeng Area

		T (°C)	pH	TDS	Alkali-nity ($CaCO_3$)	Acid-ity ($CaCO_3$)	S	Cl	F	K	S	Si
1	Shooting at 3–7 minutes interval, cloudy	85 100	8.5 9.0	1300	366	nd	20.56	50	85	194	25	93
2	Pool-clear	93	8.95	800	410	nd	15.25	42.4	78	164	24.5	109
3	Pool-clear	93	9.0	1500	252	nd	12.18	45.4	84	165	11.5	86
4	Bubbling-clear	100	9.4	1100	324	nd	20.96	37.4	97	140	21	93
5	Mixed by stream water	100	8.5	750	286	nd	7.97	41.0	80	135	11.5	74
6	Pool-clear	99.5	8.5	700	428	nd	11.27	78	85	182	22	87
7	Seeps in stream	99.5	8.45	700	370	nd	20.09	77	80	167	23	87
8	Pool-clear	80	8.0	450	392	nd	20.09	65	78	180	22	89
9	Mixed by stream water	97	8.3	400	366	nd	6.19	34	78	151	13.5	78
10	Pool-cloudy	95	8.3	400	432	nd	19.54	62	85	134	17	106

1.6.2 Hydrological Survey

It is important to estimate the amount of water recharge by precipitation to the ground water for the estimation of the geothermal reservoir and the potential amount of the recoverable geothermal fluid. It is estimated that the amount of precipitation is 150×10^4 kg/day/km^2 in the San Kampaeng area. It seems that the amount of precipitation is sufficient in this area if values are compared with other geothermal areas being developed.

The subsurface temperature is estimated by a silica thermometer and an alkaline-ratio thermometer based on the thermal water analysis done by counterpart in Thailand (Table 1.6-2).

By the analysis of the outpouring water from two springs the underground temperature is to calculated be 159°C and 160°C by the silica thermometer, 176°C and 180°C by Na-K thermometer, adn 192°C and 207°C by Na-K-Ca thermoemter.

It is considered that the wide range difference of the estimated temperature is due to the cooling of the hot water by mixing with cold ground water during upward travel from the geothermal reservoir to the ground surface, and the reaction of thermal water with rock forming minerals on the path way to the surface.

Judging from the results obtained by the geochemical thermometer, the temperature of the geothermal reservoir of the San Kampaeng area is estimated in the range of 160°C ~ 210°C.

Table 1.6-2 Chemical Composition of Hydrothermal Solution and Geochemical Thermometer in the San Kampaeng Area

Source	T (°C)	PH	Na (mg/l)	K (mg/l)	Ca (mg/l)	SiO_2 (mg/l)	Silica thermo-meter (°C)	Alkali-ratio thermometer	
								Na-K (°C)	Na-K-Ca (°C)
1	98	8.2	151	13.5	2.42	148	159	176	192
2	100	8.9	155	14.5	0.70	150	160	180	207

(after Thai's data)

1.6.3 Geochemical Survey

Geochemical survey is conducted to execute the gas concentration distribution maps for CO_2, Hg and Rn.

From the result of CO_2 survey, it is estimated that i) a high concentration area does exist in the area of geothermal manifestation, ii) a close relation exists between faults and CO_2 distribution, and iii) the geothermal activity extends to the southeast direction.

The results of Hg and Rn survey also suggest that high concentration areas are distributed in a zone from the geothermal area of manifestation to Doi Tham along the Huai Ang fault.

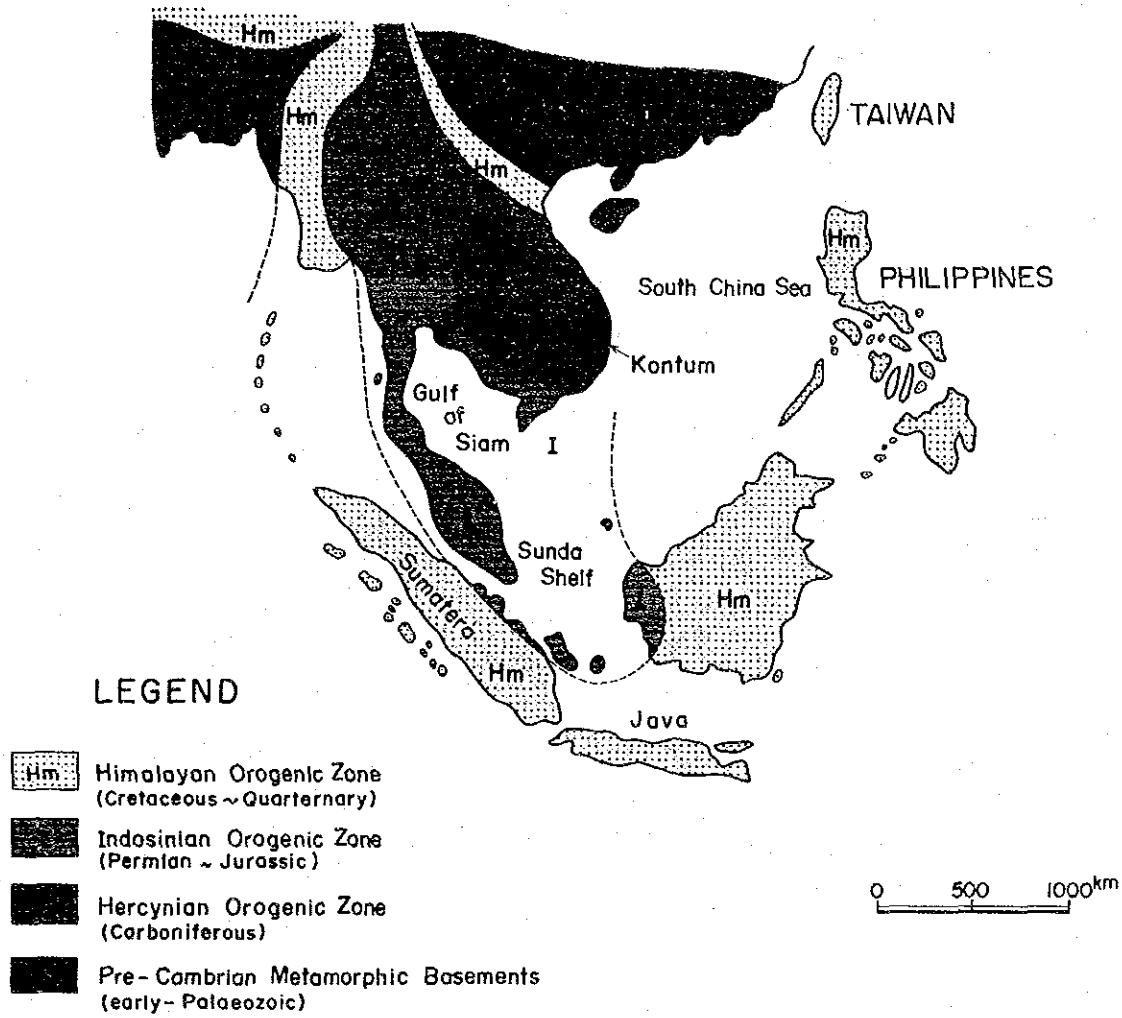

Fig. 1.1-1 Major Geological Unit of Southeast Asia